Changes in fine structure of amylopectin and internal structures of starch granules in developing endosperms and culms caused by *starch branching enzyme* mutations of *japonica* rice

Yasunori Nakamura[1,2,3,*], Akiko Kubo[3], Masami Ono[1,3], Kazuki Yashiro[4], Go Matsuba[4], Yifei Wang[5], Akira Matsubara[5], Goro Mizutani[5], Junko Matsuki[6], Keiji Kainuma[7]

[1] Starch Technologies, Co., Ltd., Akita Prefectural University, Shimoshinjo-Nakano, Akita-city, Akita 010-0195, Japan

[2] Akita Natural Science Laboratory, 25-44 Oiwake-Nishi, Tennoh, Katagami, Akita 010-0101, Japan

[3] Faculty of Bioresource Sciences, Akita Prefectural University, Shimoshinjo-Nakano, Akita-city, Akita 010-0195, Japan

[4] Graduate School of Organic Materials Engineering, Yamagata University, 4-3-16 Jonan, Yonezawa, Yamagata 992-8510, Japan

[5] School of Materials Science, Japan Advanced Institute of Science and Technology, 1-1 Asahidai, Nomi, Ishikawa 923-1292, Japan

[6] Food Research Institute, National Agriculture and Food Research Organization, 2-1-12 Kannondai, Tsukuba, Ibaraki 305-8642, Japan

[7] Science Academy of Tsukuba, 2-20-3 Takezono, Tsukuba, Ibaraki 305-0032, Japan

*Correspondence: nakayn@silver.plala.or.jp

Abstract

Cereals have three types of starch branching enzymes (BEs), BEI, BEIIa, and BEIIb. It is widely known that BEIIb is specifically expressed in the endosperm and plays a distinct role in the structure of amylopectin because in its absence the amylopectin type changes to the *amylose-extender*-type (*ae*-type) or B-type from the wild-type or A-type and this causes the starch crystalline allomorph to the B-type from the wild-type A-type. This study aimed to clarify the role of BEIIa in the culm where BEIIb is not expressed, by using a *be2a* mutant in comparison with results with *be2b* and *be1* mutants. The results showed that the amylopectin structure exhibited the B-type in the *be2a* culm compared with the A-type in the wild-type culm. The starch granules from the *be2a* culm also showed the B-type like allomorph when examined by X-ray diffraction analysis and optical sum frequency generation spectroscopy. Both amylopectin chain-length profile and starch crystalline properties were found to be the A-type at the very early stage of endosperm development at 4-6 days after pollination (DAP) even in the *be2b* mutant. All these results support a view that in the culm as well as in the endosperm at 4-6 DAP, BEIIa can play the role of BEIIb which has been well documented in maturing endosperm. The possible mechanism as to how BEIIa can play its role is discussed.

Key message BEIIb plays a specific role in determining the structure of amylopectin in rice endosperm, whereas BEIIa plays the similar role in the culm where BEIIb is absent.

Keywords Amylopectin - Culm - Endosperm - Rice - Starch branching enzyme

Introduction

Starch branching enzyme (BE) links the α-1,4-glucosidic chain onto the other acceptor chain by forming the α-1,6-glucosidic linkage. This enzymatic reaction is essential for the synthesis of amylopectin, which usually comprises 65-85% of starch. Plants have BEI and BEII types, and in addition, cereals have usually BEIIa and BEIIb isozymes (see review by Nakamura 2018). Previous studies using various mutants and transformants revealed that the impacts of three BE isozymes to the starch biosynthesis and the amylopectin structure greatly differ from each other (see reviews by Tetlow and Emes 2017; Nakamura 2015, 2018). The phenotypes of BEIIb-deficient mutants of cereals are often designated as *amylose-extender* (*ae*) because the *ae* mutant starches have apparently the high-amylose contents in the endosperm (see review by Shannon et

al. 2008). The *ae* starches in rice endosperm (Yano et al. 1985) have also modified amylopectin with more long B chains and fewer short chains of DP ≤ ca. 13 (Nishi et al. 2001). It is highly possible that the drastic changes in these starch phenotypes are due to the distinct role of BEIIb which plays an essential role in the synthesis of short chains in the region in the crystalline lamella of amylopectin cluster (Jane et al. 1997; Nakamura et al. 2020a). In contrast, the impact of loss of BEIIa activity is reportedly less significant on the fine structure of amylopectin in rice endosperm (Nakamura 2002; Sawada et al. 2018), although no detailed information on the other starch phenotypes of the *be2a* mutant has been available. The results suggest that the role of BEIIa is to support the roles of BEIIb and/or BEI in starch biosynthesis in rice endosperm. Satoh et al. (2003a) reported that the BEI mutation causes the amylopectin fine structure to have less long chains of DP ≥ 37 and more short chains of DP ≤ 10. This result suggests that the major role of BEI is to synthesize long chains of amylopectin in rice endosperm, consistent with *in vitro* studies showing that BEI has preference of longer chains whereas BEIIa and BEIIb are more reactive to short chains than long chains (Guan and Preiss 1993; Nakamura et al. 2010).

Amylopectin has a structural unit called "cluster" (French 1972) whereas glycogen has no such structural element (Thompson, 2000). The cluster of amylopectin is composed of A chains (non-branched chains) and B1 chains (branched by at least one chains) and each cluster is interconnected by long chains designated as B2 chains and/or B3 chains that span to two clusters and/or three clusters, respectively (Peat et al. 1952; Hizukuri 1986). When the non-branched segments of neighboring chains of amylopectin exceed 10 glucosyl units or degree of polymerization (DP) of 10, they form double helices (Gidley and Bulpin, 1987). The formation of double helices in amylopectin molecules profoundly affects physicochemical properties of starch granules. The cluster structure greatly affects the distinct crystalline nature of starch granules in which amylopectin molecules are packed by the lateral alignment of neighboring double helices (Kainuma and French 1972; Yamaguchi et al. 1979; French 1984). It has been reported that starch granules in cereal endosperm show the A-type crystalline polymorph whereas some tubers and rhizomes give the B-type crystalline polymorph, which have been generally distinguished by X-ray diffraction analysis (see review by Buléon et al. 1998). Although legume starches yield the C-type polymorph, which is revealed to be a mixture of A-type and B-type polymorphs (Bogracheva et al. 1998). The A-type starch is composed of a monoclinic unit cell whereas the B-type starch has a hexagonal unit cell, and thus the A-type starch is more densely packed than the B-type starch (see review by Imberty et al. 1991).

It has been established that starch is synthesized in concerted actions of starch synthase (SS), BE, and starch debranching enzyme (DBE). Although three starch biosynthetic enzyme have multiple isozymes, their roles and expressions in various organs and tissues are totally different in rice (Ohdan et al. 2005). For example, BEIIb is almost specifically expressed in the endosperm

while BEIIa and BEI are ubiquitously present in rice plants (Yamanouchi and Nakamura 1992). Culm is one of vegetative organs in rice plants, where a great amount of starch is accumulated, particularly before the anthesis, but subsequently the stored starch in the culm is quickly degraded to sucrose and translocated to the kernel to support its productivity (Horie et al. 2005).

In the present study, to investigate the contribution of each BE isozyme to starch biosynthesis in endosperm and culm of rice, the fine structure of amylopectin was examined by using *be2a*, *be2b*, and *be1* mutants generated from *japonica*-type rice. Past biochemical and genetic investigations have established that mutations in *BEIIb* gene alter the A-type crystallinity of their starches to the B-type starches in endosperms of maize (Gérard et al. 2000) and rice (Nishi et al. 2001; Tanaka et al. 2004), whereas no such changes have been observed in the *be1*- and *be2a*-mutants (Satoh et al. 2003a; Nakamura, 2018). Therefore, we tried to clarify the contribution of BE isozymes to the amylopectin fine structure and the starch granule crystalline structures in endosperm and culm. The structural features of amylopectin from these *be* mutants were analyzed and compared with those of its wild-type Kinmaze and/or Taichung65 in details. The internal starch granule structures were also examined using wide angle X-ray diffraction (XRD), solid-state ^{13}C NMR (Gidley and Bociek 1985; Flanagan et al. 2013), and sum frequency generation spectroscopy (SFG) (Miyauchi et al. 2006; Kong et al. 2014).

Materials and methods

Reagents

A fluorophore 8-amino-1,3,6-pyrenesulfonic acid (APTS) was purchased from AB SCIEX (Tokyo, Japan). The standard glucans, BD4A and BD4B, were prepared according to the procedures reported previously (Matsuki et al. 2019). Nägeli amylodextrin was prepared by incubating waxy rice starch (Mochiru B, Joetsu Starch Co. Ltd., Niigata, Japan) in 16 % H_2SO_4 at 37 °C with agitation at 60 rpm for 35 days. Linear and branched dextrins were fractionated using pyridine-methanol precipitation according to the method by Kikumoto and French (1983). The branched fraction was further purified by repeated recrystallization in cold 10% ethanol to obtain BD4. BD4 was recrystallized in 16 M methanol to obtain BD4A or recrystallized in 10% ethanol for BD4B. The precipitate was collected by centrifugation, washed in methanol for BD4A or in water for BD4B, and air-dried.

Plant materials and sampling

Rice BE-related mutant lines, a *be2a* mutant line EM19, a *be2b* mutant line EM10, and a *be1* mutant line EM557, were generated by treating fertilized egg cells of *japonica*-type cultivars Kinmaze (for EM19 and EM10) and Taichung65 (for EM557), as described previously by Satoh et al. (2003b). Rice plants were grown in the experimental field of Akita Prefectural University under natural environmental conditions during summer months. Several hundreds of panicles having developing seeds at various days after pollination (DAP) were harvested in the early afternoon in sunny days from randomly chosen rice plants and stored at -80°C before use. Mature seeds were also harvested, dried, and kept at 10°C before use. Culms were harvested just before the anthesis and stored at -80°C before use.

Preparation of enzyme extracts from rice developing endosperm and culm

Five randomly selected developing rice kernels at 15-20 DAP were homogenized in a plastic tube by hand by using a plastic pestle on ice with 250 µl of a grinding solution (GS) including 50 mM imidazole-HCl (pH 7.4), 8 mM $MgCl_2$, 5 mM dithiothreitol, and 12.5% (v/v) glycerol. The homogenate was centrifuged at 10,000 g for 20 min at 4°C. The supernatant was centrifuged again under the same condition. The resulting supernatant was designated as the enzyme extract and used for native-PAGE/BE activity staining analysis.

About 1 g (fresh weight) of the randomly selected culms harvested and pooled from about 5 individual plants was cooled in liquid nitrogen and homogenized with a mill (Model A11B5001, IKA-Werk GmbH & Co. KG, Staufen, Germany) which had been cooled in liquid nitrogen. The powder was again homogenized with mortar and pestle which had been cooled in liquid nitrogen. About 15-25 mg of the powder was homogenized with 3.7 volume of GS. The enzyme extract used for zymogram was prepared in the same procedures as those for the preparation of the enzyme extract from developing kernels, as stated above.

Native-PAGE/BE activity staining of rice developing endosperm and culm

Native-PAGE/BE activity staining method was conducted to measure BEI, BEIIa, and BEIIb in developing endosperm and culm, according to the procedure reported previously (Yamanouchi and Nakamura 1992), except that 1.0 µg oyster glycogen (type II, SIGMA) was included in 1.0 ml of the resolving gel.

Preparation of starch granules from rice endosperm and culm

Starch granules from mature endosperm and culm were prepared as described previously (Nakamura et al. 2020a). Starch granules from developing endosperm were soaked in methanol at -80°C for about 3 days and then stored at -30°C for additional 7-10 days before use. For preparation of starch granules in the endosperm at the very young stage (4-6 DAP) and mid-milky stage (15-20 DAP), arbitrary chosen approximately 80 seeds at 4-6 DAP and 30 seeds at 15-20 DAP were dehulled with scissors and forcepts and the endosperm sap was gently squeezed and suspended in approximately 5 ml of 80% (v/v) ethanol solution so that the green pericarp was removed. The suspension was filtered through a nylon net (pore size, 100 μm), and the filtrate was centrifuged at 3,000 g for 15 min at 20°C. The precipitate was mixed with 5 ml of 10% (v/v) ethanol and centrifuged. The precipitate was added by 0.5 ml of 10% (v/v) ethanol and the mixture was layered onto 1.0 ml Percoll solution (MP Biochemicals, LLC., Illkirch, France) in a 2.0-ml plastic tube. The tube was centrifuged at 8,000 g for 20 min at 20°C, and the precipitate was washed twice with 1 ml of 10% ethanol. The washed precipitate (approximately 10-15 mg from the 4-6 DAP endosperm) was dried in vacuum and stored at -20°C until used. Starch granules in the culm from Kinmaze and EM19 were prepared as described above, although the starch sample was washed with toluene before the use of Percoll precipitation to remove proteins.

Chain-length distribution analysis of amylopectin

The chain-length distribution of amylopectin was analyzed by using the fluorophore-assisted carbohydrate electrophoresis (FACE) method (O'Shea et al. 1998) after treatment of amylopectin with *Pseudomonas amyloderamosa* isoamylase, followed by labelling of APTS at the reducing ends of debranched glucan chains, as described previously (Nakamura et al. 2020a).

Measurement of amylose content by gel filtration chromatography of starch treated with isoamylase

The amylose content of *Pseudomonas amyloderamosa* isoamylase-debranched starch in the culm from Kinmaze and EM19 was determined as described previously (Toyosawa et al. 2016).

X-ray diffraction pattern analysis of starch granules

XRD measurements were performed on a Nano-viewer system (Rigaku Co., Tokyo, Japan) at a wavelength of 0.154 nm (CuKα). The camera lengths were 110 mm. A Pilatus 1M (Dectris AG, Baden, Switzerland) detector was used, with a q range of 3.5 to 25 nm^{-1}; q is the magnitude of the scattering vector and is defined as follows:

$q = 4\pi \sin\theta \ /\lambda$ (1),

where 2θ and λ are the scattering angle and wavelength, respectively. The starch granule samples were put into the sample cell of approximately 500 μm thickness. Data processing, which included controlling the contrast of the 2D-patterns and the preparation of a 1D-profile from the obtained 2D-patterns, was performed using the FIT-2D software (Ver. 12.077, Andy Hammersley/ESRF, Grenoble, France).

Optical sum frequency generation (SFG) spectroscopy of starch granules

For scattered SFG measurement the powder samples of EM10 and Kinmaze were put in transparent silica glass square cells (AS ONE Q-101) of sizes 3.5 mm × 12.5 mm × 45 mm. The internal sizes of the cells were 1mm in thickness and 10mm in width. We put an aluminum frame in the cell and made an empty space of sizes 0.9 mm × 2 mm × 7 mm in the center of the cell. We put our powder sample into this space and observed its SFG through the glass window of the cell. The SFG spectroscopy system was already described previously (Hieu et al. 2015; Nakamura et al. 2020a). Tunable infrared light pulses at wavelength of approximately 3 mm was output from an optical parametric generator (EKSPLA PG401/DFG2-18P) pumped by the fundamental and third harmonic output of a Nd^{3+}:YAG laser (EKAPLA PL2143B) with time width 30 ps and repetition rate of 10 Hz. The pulse energy of the visible light was about 10 mJ and that of the infrared (IR) was about 260 mJ at the sample. The spectral width of the IR light was 6 cm^{-1}. More details are the same as those described in our previous paper (Nakamura et al. 2020a).

Results

Native-PAGE activity staining of BE isozymes in developing endosperm of *be* mutants of rice

In the present study, three different *be* mutant lines of *japonica* rice were used; a *be2a* mutant line EM19, a *be2b* mutant line EM10, and a *be1* mutant line EM557, whereas their parent wild-type cultivars were Kinmaze for EM19 and EM10 and Taichung65 for EM557 (Satoh et al. 2003b). The native-PAGE activity staining method was used to detect the activity of each BE isozyme in plant materials used in this study. Fig. 1a shows that the activity of BEIIa was deficient in developing endosperm from EM19, although a low BEIIa activity still remained in the endosperm. The activities of BEIIb and BEI were lacking in endosperms from EM10 and EM557, respectively. BEIIa accounted for the most BE activity in the culm from Kinmaze, whereas a significant BEI

activity was present, although no BEIIb activity was found (Fig. 1b). It was found that no activities of BEIIa and BEI were detected in the culms from EM19 and EM557, respectively (Fig. 1b). The results indicate that these mutant lines as well as their parent cultivars were useful to examine the roles of three BE isozymes in starch biosynthesis in the endosperm and culm.

Chain-length distribution of amylopectin in developing endosperm at 4-6 DAP and 15-20 DAP of *be* mutants of rice

Our previous studies established the effects of loss in activities of individual BE isozymes on the chain-length distribution of amylopectin in mature endosperm of *japonica* rice (Nakamura 2002, Nishi et al. 2001; Satoh et al. 2003a). In this study, we analyzed the chain profiles of amylopectin in developing endosperms at the very early developing stage (4-6 days after pollination, DAP) and the milky stage (15-20 DAP) in every *be* mutant line, as well as that in Kinmaze. When BEIIb was lacking in the EM10 endosperm at 15-20 DAP, amylopectin had much more long chains of DP ≥ approximately 37 and significantly more intermediate chains of about 15 ≤ DP ≤ about 30, but depleted short chains of DP ≤ approximately 13 (Figs. 2b and 2f). This change was very similar to that in amylopectin chain profile in mature EM10 endosperm, as reported previously (Nishi et al. 2001). In contrast, however, in the very young EM10 endosperm at 4-6 DAP, the extent of such changes in amylopectin chain-length was much smaller than that in the 15-20 DAP endosperm (Figs. 2e). In fact, the chain-length pattern of the EM10 4-6 DAP endosperm amylopectin was very similar to the wild-type one (Figs. 2a-c), which was greatly different from that of the EM10 DAP15-20 endosperm amylopectin (Fig. 2d).

Based on the previous and present results, we define the rice amylopectin structure in two types in the present paper. The A-type amylopectin is usually found in wild-type endosperm whereas the B-type amylopectin is synthesized in the *be2b* mutant endosperm. The A-type amylopectin has more short chains of DP 6-12 and fewer long chains of DP ≥ 37 than the B-type amylopectin and starch granules composed of the A-type amylopectin show the A-type crystalline allomorph whereas those including the B-type amylopectin exhibit the B-type allomorph.

Chain-length distribution of amylopectin in the culm of *be* mutants of rice

Amylopectin in the culm from Kinmaze showed the similar chain length distribution pattern to that in the endosperm, with exceptions that a small amount of very short chains of DP 3-5 were included in the culm amylopectin and that the proportion of the DP 8 chain was lower than that of the DP 6-7 chains (Fig. 3a). The former exceptional observation suggests that amylopectin side chains are partially degraded by amylases and phosphorylase in the culm, while the latter suggests

that the activity of SSI which is considered to play a specific role in elongating the DP 6-7 chains to form the DP 8 chain (Fujita et al. 2006: Nakamura et al. 2014) is lower in the culm than that in the endosperm. This idea seems to be consistent with the recent report by Morita et al. (2019) that the relative SSI activity is much lower in rice leaf sheath than that in the endosperm. In the EM19 culm, the proportion of long chains of DP ≥ 37 (the B2-4 chains) as well as intermediate chains was markedly higher while that of short chains was apparently lower (Fig. 3b). The observation was clearly shown in Fig. 3f when the chain profile of EM19 amylopectin was subtracted by the Kinmaze (the parent wild-type cultivar) amylopectin in the culm, and this figure demonstrates that the pattern of difference was almost the same as that between EM10 and Kinmaze amylopectin in the culm (Fig. 2f). In contrast, however, no significant change was observed in the EM10 and EM557 in their culm amylopectin compared with Kinmaze (Fig. 3c-e). These results show that the contribution of BEI to the amylopectin structure is minor or its role is easily complemented by BEIIa, and that the EM10 amylopectin must be the same as the Kinmaze amylopectin because BEIIb is not expressed in the culm even in Kinmaze, as shown in Fig. 1b.

The most striking observation in Fig. 3 is that the amylopectin structure in the EM19 culm was considered to become the *ae*-amylopectin-type, namely the B-type. This strongly suggests that BEIIa plays an essential role in amylopectin biosynthesis and its structure in the culm as BEIIb in the endosperm whereas the role of BEIIa seems to be only limited in the endosperm because in its absence no significant change happens in the amylopectin structure in EM19 mutant (Nakamura 2002). It is known that starch granules having *ae*-amylopectin like in EM10 endosperm exhibits the B-type allomorph (Nishi et al. 2001; Tanaka et al. 2004). This observation led us to examine the crystalline allomorphs of starch granules in the EM19 culm by XRD and SFD.

The amylose content and amylopectin chain profile in the culm of *be2a* mutant of rice

The effect of deficiency of BEIIa activity on the amylose content as well as the amylopectin chain profile in the culm were examined by using gel filtration chromatography of isoamylase-debranched starch. The amylose contents including extra-long chains of amylopectin, if any, in the culm were approximately 20% and 30% of the starch in Kinmaze and EM19, respectively (Fraction I in Fig. 4). It was also found that the ratio of the amount of Fraction III (A plus B1 chains) to that of Fraction II (B2-4 chains) was apparently higher in Kinmaze than EM19, consistent with the results of chain-length distribution analysis (compare Fig. 3a with Fig. 4b).

X-ray diffraction (XRD) patterns of starch granules in endosperm and culm of *be* mutants of rice

Wide angle X-ray diffraction (XRD) measurements can distinguish the A-type allomorph from the B-type allomorph of the internal starch granule structure. Figure 5 shows the XRD profiles of standard glucans, BD4A and BD4B, and starch granules in mature endosperms of Kinmaze, EM10, EM19, and EM557. The XRD profile of BD4A (Fig. 5a) had peaks at the scattering vector, q, of approximately 10.58 (a single peak), 12.03 and 12.71 (doublet peaks), and 16.18 nm^{-1} (a single peak), which are characteristics of A-type starch granules in cereal endosperm. On the other hand, the XRD profile of BD4B (Fig. 5a) had peaks at q of approximately 3.724 (a single peak), 11.38 (a single peak), 15.54 and 16.92 nm^{-1} (doublet peaks). The starch granules in mature endosperms of Kinmaze (Fig. 5b), Taichung-65 (Fig. 5c), EM19 (Fig. 5d), and EM557 (Fig. 5f) consisted of mainly A-type crystal, while those of EM10 (Fig. 5e) consisted B-type crystal (Nakamura et al. 2020a; Nagasaki et al. 2021).

Figures 6 shows the XRD patterns of starch granules in 4-6 DAP endosperm, 15-20 DAP endosperm and the culm. The starch granules of Kinmaze in 4-6 DAP endosperm, 15-20 DAP endosperm and culm were found to be assigned as A-type crystals (Figs. 6a, 6b, and 6c, respectively). However, the starch granules of EM10 endosperm were quite different from those of Kinmaze endosperm. In the starch granules of EM10 endosperm at 4-6 DAP, we could not find the peak at q = 3.724 nm^{-1}, which is characteristic peak of B-type crystal, while the peak at 12.03 nm^{-1} and the shoulder of 12.71 nm^{-1} were observed (Fig. 6d). From these results, starch granules in EM10 endosperm at 4-6 DAP consisted of A-type crystals. Furthermore, we could see the XRD peaks for starch granules in EM10 endosperm at 15-20 DAP at q = 3.724 nm^{-1} (weak) and q = 12.03 nm^{-1} and the shoulder of 12.71 nm^{-1} (Fig. 6e). These results suggest that these starch granules had mixed A-type and weak B-type crystals, called B'-type crystal. The starch granules in EM19 culm were quite different from A-type and B-type crystals (Fig. 6f). The broad peak positions were q = 3.9, 12.2 and 15.7 nm^{-1}. These peaks were coincident of several B-type crystal diffraction peaks. This result suggests the precursor of B-type crystals, being similar to liquid-crystalline-type precursors of polymer crystals (Henmi et al. 2016; Chonan et al. 2021).

Optical sum frequency generation (SFG) spectroscopy of starch granules in endosperm and culm of *be* mutants of rice

We show SFG spectra obtained for starch granules in mature endosperms of Kinmaze, EM10, EM19, EM557, standard mature rice BD4A and BD4B in developing endosperms (4-6 DAP and 15-20 DAP) of Kinmaze and EM10, and in culms of Kinmaze and EM19. Figure 7 shows the

ones in mature endosperms. Big peaks at around 2910 cm^{-1} and 2970 cm^{-1} were assigned to C-H and C-H_2 stretching vibrations, respectively. The broad peak around 3100cm^{-1} was tentatively assigned to H_2O peak in our previous paper (Nakamura et al. 2020a). The shoulder peaks at 2860 cm^{-1} seen in some of the spectra may be assigned to CH_2 vibration. There were clearly two distinct types of SFG spectra, namely, BD4A (Fig. 7a), Kinmaze (Fig. 7c), EM19 (Fig. 7d), and EM557 (Fig. 7f) gave similar spectral shapes to each other and they were consistent with the spectral shapes of A-type amylopectin as they were reported by Kong et al. (2014) and Nakamura et al. (2020a). BD4B (Fig. 7b) and EM10 (Fig. 7e) gave similar spectral shapes to each other and they were consistent with those of B-type amylopectin.

Figure 8 shows SFG spectra of amylopectin in immature endosperms, namely, in endosperms of 4-6 DAP and 15-20 DAP of Kinmaze (Fig. 8a and 8b, respectively) and EM10 (Fig. 8d and 8e, respectively). The figure also shows the SFG spectra of amylopectin in the culms of Kinmaze and EM19. It was not easy to classify the spectra into two groups. From Fig. 8 we see that the SFG spectra of A-type amylopectin had characteristic features of 1) 2910 cm^{-1} and 2970 cm^{-1} peaks of almost equal height, 2) deep dips at 2950cm^{-1} together with the bigger broad peak at 3100cm^{-1}, and 3) 2910 cm^{-1} peak with a rather broad top. The characters 1) and 3) were only seen for the Kinmaze culm. The character 2) was seen in endosperm starches from Kinmaze (4-6 DAP) (Fig. 8a), Kinmaze (15-20 DAP) (Fig. 8b), and EM10 (4-6 DAP) (Fig. 8d).

The SFG intensity was fit to Lorentzian curved in Eq. (1) below and fitting parameters were obtained as shown in Supplementary Table S1.

$$|\chi^{SFG}|^2 = \left|\chi^{NR} + \sum_{n=1}^{5} \frac{A_n \exp(i\theta_n)}{\omega - \omega_n + i\gamma_n}\right|^2 \qquad (1)$$

However, it was not easy to get any tendency from the table. Hence the spectral shapes in Figs. 7 and 8 were analyzed by the principal component analysis (PCA). The results were shown in Supplementary Fig. S1. The PCA program did not output the physical meaning of the two axes, but we could speculate by comparing Supplementary S1 with Figs. 7 and 8. Then the horizontal axis (PC1) mainly is considered to represent the intensity ratio of the two big peaks at 2910 cm^{-1} and 2970 cm^{-1} and the dip depth at 2950 cm^{-1}. The vertical axis (PC2) is considered to represent the noise amplitude in the data. So here, PC2 is disregarded from consideration, and only PC1 is considered. In Supplementary Fig. S1, the data points are distributed almost continuously, so it is difficult to classify them. However, we dare to make three groups as:

(1) a group including BD4B, EM10, EM10 (15-20) distributed for PC1 < -0.5

(2) a group including EM19 (culm), BD4A, EM10 (4-6) distributed for -0.5 < PC1 < 0

(3) a group including Kinmaze (15-20 DAP), Kinmaze (4-6 DAP), EM19, EM557, Kinmaze (culm) distributed for PC1 > 0.

The three members in group (1) seen in Figs. 7 and 8, i.e. BD4B, EM10, and EM10 (15-20 DAP) had similar spectral shapes to each other and one of them was BD4B, and so the group was

considered to be the B-type. Kinmaze at PC1 = 0.8 in group (3) was known to be of the A-type, and so the group (3) with 6 members could be classified as of the A-type. BD4A at PC1 = -0.2 in group (2) was known to be the A-type, and so the group (2) could be classified as the A-type. However, the SFG spectra of EM19 (culm) and EM10 (4-6 DAP) classified in (2) were likely to be the B-type in Fig. 8. Therefore, the group (2) might be a mixture of A-type and B-type. It was a little controversial that BD4 (A) in (2) was judged to be a mixture of A- and B-types, and it should be checked repeatedly in future analyses.

Discussion

Cereals supports the world population by providing staple food. In cereals three BE isozymes, namely BEI, BEIIa, and BEIIb, are present playing distinct roles in starch biosynthesis (see reviews by Nakamura 2015, 2018). Cereals store a large amount of starch in their endosperms. Three BE isozymes differently contribute to the fine structure of amylopectin. It is known that there are two types of branch linkages in amylopectin molecules, differing in their positions at the cluster, a structural element of amylopectin (Jane et al. 1997; Nakamura et al. 2020a). It is considered that in rice endosperm amylopectin the first type branches are present in the amorphous lamellae of the cluster and formed mainly by BEI, whereas the second type branches are localized in the basal region (the reducing side) of the crystalline lamellae of the cluster or intermediate region between the crystalline and amorphous lamellae and are almost exclusively synthesized by BEIIb (Nakamura et al. 2020a), as illustrated in Fig. 9. The present study aimed to examine contributions of three BE isozymes to the fine structure of amylopectin and the internal structures of starch granules in developing endosperm and culm by using a *be2a* mutant line, EM19, a *be2b* mutant line, EM10, and a *be1* mutant line, EM557.

The role of BEIIb in the starch biosynthesis in rice endosperm

In rice plants, BEIIb is specifically expressed in the endosperm, affecting the structural features of amylopectin and crystalline properties of starch granules (Nishi et al. 2001; Nakamura 2018; Nakamura et al. 2020a). When BEIIb is defective in the endosperm, chain-lengths of side chains of amylopectin became longer (Fig. 2), resulting in elongated lengths of double helices, and this caused starch granules to be resistant to gelatinization and shifted the crystalline allomorphs to the B-type from the A-type, as determined by XRD (Fig. 5) and SFG analyses (Fig. 7), consistent with our recent studies (Nakamura et al. 2020a) and past investigations by other groups worldwide (Wei et al. 2010; Butardo et al. 2011).

What are the structural features in the amylopectin fine structure and starch granular structures at the very early developmental stage of endosperm? In this study, we examined these features at 4-6 DAP and 15-20 DAP and compared them with each other and with those in mature endosperms. In such an early developmental stage, the endosperm includes very fine starch granules (Matsushima et al. 2015, 2016) and more malto-oligosaccharides and dextrins (Nakamura et al. 2020b). It is also known that the activity of BEIIa is high whereas BEIIb is scarcely expressed in this stage (Ohdan et al. 2005).

At 4-6 DAP, both the chain-length distribution pattern of amylopectin and crystalline allomorph of starch granules in EM10 were A-types (Figs. 2 and 6), in contrast with the results that in mature EM10 endosperm they were typically B-types (Fig. 5). However, amylopectin in the 15-20 DAP endosperm from EM10 was clearly a B-type (Fig. 2), being the same as that in mature endosperm (Fig. 10). The crystalline allomorph of starch granules in the 15-20 DAP endosperm from EM10 was also like the B-type by the XRD analysis, although its XRD pattern was not an apparent B-type one as observed in starch granules in mature EM10 endosperm (compare Fig. 6 with Fig. 5). This trend was basically the same as in the SFG analysis (Figs. 7 and 8), although further analyses are needed in future, as described above.

These results indicate that the change in amylopectin fine structure does not necessarily related to that in internal structures in starch granules. Considering that young endosperms contain small developing starch granules (Matsushima et al. 2015, 2016), it is highly possible that the degree of crystallinity of starch granule depends on the maturity of starch granules in developing endosperm.

There have been numerous investigations using BEIIb-related mutants and transformants in which BEIIb activity was inhibited in rice endosperm (see reviews by Nakamura 2018; He and Wei 2020). Wei and his colleagues examined in details the effects of deficiency of BEIIb on starch biosynthesis in endosperm of rice and other cereals and revealed many interesting results, although most of their results were obtained by using *be2b/be1* double mutants and transformants and thus it is unclear if these starch-related phenotypic changes were caused by loss of activity of only BEIIb or that of both BEIIb and BEI (He and Wei 2020). They reported heterogenous starch granules in the *be2b/be1* endosperm, because they included both A-type and B-type starches in the same starch granules and thus they were called C-type starches (Wei et al. 2010). They also proposed the existence of biphasic starch granules in these lines (He et al. 2018; He and Wei 2020). They explained that the starch granules at the very early developmental stages are composed of A-type starch, but with the elapse of the maturation they include the B-type starch in the outer region of the enlarged granules, whereas A-type starches remain the same type in the inner region of the granules. The phenomena seem to be consistent with the present observations with the *be2b* mutant EM10, as described above (Figs. 2, 6, and 8).

The role of BEIIa in the starch biosynthesis in rice culm

Although BEIIb gives a strong impact to the amylopectin structure and the starch granular structures of the endosperm, it is not present in the culm of rice (Fig. 1). Instead, BEIIa accounted for the major BE activity whereas BEI activity was significantly present in the culm (Fig. 1). Thus, BEIIa and BEI are involved in starch biosynthesis in the culm. In the culm of wild-type Kinmaze the amylopectin chain-length distribution showed an A-type pattern. On the other hand, amylopectin in EM19 culm had enriched long chains of DP≥37 and depleted short chains of DP6-14, the pattern being a typical B-type amylopectin one (Fig. 3). These results were also supported by the gel filtration analysis of debranched culm starches from Kinmaze and EM19 (see the ratio of Fraction III/Fraction II in Fig. 4). In the *be2a* mutant culm the starch granules also possessed a characteristic B-type pattern when analyzed by XRD (Fig. 6) and SFG (Fig. 8), although these profiles were not apparent as those detected in the starch granules in EM10 endosperm (compare with Figs. 5 and 7).

The results strongly suggest that BEIIa has an impact on the amylopectin structure in rice culm as BEIIb does in rice endosperm. It is thought that BEIIa plays an essential role in the synthesis of short chains of amylopectin in the culm. Therefore, in the absence of BEIIa, the amylopectin fine structure and starch granular structure became B-types in the culm instead of A-types of those in the wild-type culm (Figs. 3, 6, and 8). However, why the XRD pattern of starch granules from the *be2a* mutant culm did not show distinct B-type one (Fig. 6)? Firstly, the fine structure of amylopectin from the *be2a* culm might have a lower B-type structure compared with that from the *be2b* endosperm. Secondly, the crystallinity of starch granules in the culm might be lower than that in the endosperm. Fig. 10 compares the chain-length pattern of amylopectin between the *be2b* endosperm and the *be2a* culm. Surprisingly, the impact of loss of BEII isozymes to the amylopectin structure was stronger in the *be2a* culm than in the *be2b* endosperm. The results strongly suggest that the contribution of BEIIa to the amylopectin structure in the culm is rather stronger than that of BEIIb in the endosperm. Thus, the first possibility is unlikely, but the second possibility might be the case. The amylose content in the culm starch was approximately 20% and 30% in Kinmaze and EM19, respectively (Fig. 4). Therefore, it is unlikely that a high amount of amylose is a major factor which hampers the crystallinity of the starch in EM19, although the possibility that amylose affects the crystallinity of starch granules to some extent in the EM19 culm cannot be excluded. To resolve these problems needs further analyses by using a large amount of starch granules purified from both tissue and organ.

The contributions of BEIIa and BEIIb to the fine structure of amylopectin and the internal structure of starch granules in rice endosperm and culm

Table 1 summarizes the types of amylopectin fine structure and internal structures of starch granules in endosperm and culm of various *be* mutants and the wild-type. BEIIb determines the amylopectin structure and the crystalline allomorphs of starch granules. In rice endosperm the contribution of BEIIb is specific and this cannot be complemented by BEIIa and BEI although their activities are present in developing endosperm at the comparative levels as that of BEIIb activity (Fig. 1).

BEIIa is ubiquitously expressed in rice tissues (Yamanouchi and Nakamura 1992). It has been reported that the role of BEIIa in starch biosynthesis seems to be minor in developing endosperm because no significant change in starch phenotype is detected in mature endosperm when BEIIa activity is lacking and the role of BEIIa is only slightly observed in the absence of both BEIIa and BEIIb (Nakamura 2002; Sawada et al. 2018). However, the present study showed that in the culm where BEIIb was not expressed, the role of BEIIa was apparent in the culm. The chain-length distribution analysis of amylopectin clearly indicates that its fine structure was the A-type in the presence of BEIIa (the wild-type cultivar, Kinmaze) whereas it was the B-type or *ae*-type in the absence of BEIIa (the *be2a* mutant line, EM19) (Fig. 3). The results were consistent with the gel filtration chromatography analysis indicating that the ratio of the amount of short and intermediate chains (A plus B1 chains belonging to Fraction III) to long chains (B2-4 chains belonging to Fraction II) was clearly higher in starch in the culm from Kinmaze than that in EM19 (Fig. 4). The internal crystalline structure of starch granules in the culm also changed from the A-type in Kinmaze to the B-type in EM19 (Figs. 6 and 8). To what extent is BEIIa responsible for the change in amylopectin fine structure? A balance of total BE to SS activities might influence the amylopectin structure. Firstly, past investigations indicate that although any kinds of rice mutants affect the BE/SS activity balance, the dramatic alteration of endosperm amylopectin structure to B-type was only found in *be2b* mutants and transformants (see review by Nakamura 2018). Secondly, Sawada et al. (2018) reported that the chain-length distribution pattern of amylopectin was only slightly changed in rice endosperm from the BEI/BEIIa suppressed line, whereas it was markedly altered in endosperm from the BEI/BEIIb and BEIIa/BEIIb suppressed lines. These results strongly suggest that change of the amylopectin structure from A-type and B-type was mainly caused by decrease of BEIIb activity in the endosperm or by that of BEIIa activity in the culm, whereas contribution of a low ratio of total BE to SS activities to this type of change is limited.

How could BEIIa play a role in starch biosynthesis in the culm in the same manner as BEIIb does in the endosperm? Crofts et al. (2015) reported that BEIIb is responsible for the formation of a variety of protein-protein macromolecular complexes with other starch biosynthetic isozymes such as BEI, BEIIa, SSI, and SSIIa in developing rice endosperm. One explanation might be that

BEIIa is inactive during starch synthesis inside the multi-protein complexes in developing endosperm. In the culm, the formation of the protein complexes would be largely restricted due to the absence of the BEIIb protein and other proteins involved in starch biosynthesis which are presumably present at much higher levels in developing endosperm than in the culm (Nakamura et al. 1989). This possibility needs to be examined by the future study.

The observations that both the amylopectin structure and starch granular structures were seemingly A-types even in the *be2b* mutant line, EM10, at the 4-6 DAP endosperm (Figs. 2, 6, and 8) might be explained by the same way. At such very early developmental stage, BEIIa can function even in the endosperm because many starch synthesis-related proteins are present at lower levels compared with the later maturing stages, and thus BEIIa can be free from restriction of its activity by other proteins. If this possibility is the case, the regulatory mechanism for the starch biosynthesis differs between the very early developmental stage and the later maturing stage of the endosperm. This might be related to our previous observations that patterns of transcripts of starch biosynthetic enzyme genes (Ohdan et al. 2005) and the distribution and levels of malto-oligosaccharides (Nakamura et al. 2020b) greatly different between the endosperm developmental stages.

Conclusions

The present study confirmed the specific role of BEIIb in starch biosynthesis in maturing endosperm of rice by the formation of short outer chains within the amylopectin cluster. Thus, in its absence both the amylopectin fine structure and the internal starch granular structure became B-types in mature endosperm, in contrast with A-types found in wild-type. However, at the very early developmental stage of the endosperm at 4-6 DAP, the amylopectin chain-length pattern showed the A-type in all *be* mutant lines as well as wild-type, suggesting that amylopectin was synthesized to have the A-type structure in different way at this stage from that at the later maturing endosperm stage, consistent with the previous studies reported by the Wei's group (see review by He and Wei 2020).

What is the role of BEIIa in other tissues, whereas in maturing endosperm its role seems to be masked by the contribution of BEIIb to starch structures? The present results showed that the amylopectin structure shifted to the B-type in the culm of the *be2a* mutant from the A-type in wild-type, indicating that BEIIa contributes to the amylopectin structure in the culm in the same manner as BEIIb in the endosperm. The distinct structural change in amylopectin in the *be2a* culm caused an alteration of the starch granular structure to the B-type crystalline allomorph in the mutant in contact with the A-type in the wild-type. In what way BEIIa could function in the culm

in spite of its inability in maturing endosperm? One simple explanation is that the inability of the BEIIa function in maturing endosperm might be due to restriction of its activity by association with other starch biosynthetic proteins, whereas BEIIa could plays a role in the synthesis of short cluster chains of amylopectin, free from the association with other proteins.

In conclusion, the present investigation provided new insights into the contributions of BEIIa and BEIIb to starch biosynthesis in endosperm and culm of rice.

Acknowledgements We thank Dr. Hikaru Satoh for providing us with rice mutants used in this study. We also thank Dr. Naoko Fujita for help to use facilities in Akita Prefectural University, and Dr. Satoko Miura for instruction of the method for measurement of amylose content of the starch sample. This study was funded by JSPS KAKENHI Grant Number JP19H05721 (GMa).

Author contribution YN conceived and designed the study. Those who conducted the research and analyzed the data were YN, AK, and MO (biochemical experiments), KY and GMa (XRD), and YW, AMa, and GMi (SFG). JM prepared standard glucans, BD4A and BD4B, whereas YN prepared glucans from rice. YN, JM, KK, GMa, and GMi wrote, read and approved the manuscript.

Conflict of interest The authors declare that they have no competing interests.

References

Bogracheva TY, Morris VJ, Ring SG, Hedley CL (1998) The granular structure of C-type pea starch and its role in gelatinization. Biopolymers 45:323-332

Buléon A, Colonna P, Plachot V, Ball S (1998) Starch granules: Structure and biosynthesis. Int J Biol Macromol 23:85-112

Butardo VM, Fitzgerald MA, Bird AR, Gidley MJ, Flanagan BM, Larroque O et al (2011) Impact of down-regulation of starch branching enzyme IIb in rice by artificial microRNA- and hairpin RNA-mediated RNA silencing. J Exp Bot 62:4927-4941

Chonan Y, Matsuba G, Nishida K, Hu W (2021) Crystal methodology of polyurea on rapid quenching. Polymer 213:123201

606 Crofts N, Abe N, Oitome NF, Matsushima R, Hayashi M, Tetlow IJ et al (2015) Amylopectin
607 biosynthetic enzymes from developing rice seed form enzymatically active protein complexes.
608 J Exp Bot 66:4469-4482
609 Flanagan BM, Gidley MJ, Warren FJ (2013) Rapid quantification of starch molecular order
610 through multivariate modelling of ^{13}C CP/MAS NMR spectra. Chem Commun
611 French D (1972) Fine structure of starch and its relationship to the organization of starch granules.
612 J Japan Soc Starch Sci 19:8-25
613 French D (1984) Organization of starch granules, in Starch: Chemistry and Technology, ed.
614 Whistler RL, BeMiller JN, Paschall E, Second Edition (San Diego, New York, Boston,
615 London, Sydney, Tokyo, Toronto: Academic Press), pp. 183-247
616 Fujita N, Yoshida M, Asakura N, Ohdan T, Miyao A, Hirochika H, Nakamura Y (2006) Function
617 and characterization of starch synthase I using mutants in rice. Plant Physiol 140:1070-1084
618 Gérard C, Planchot V, Colonna P, Bertoft E (2000) Relationship between branching density and
619 crystalline structure of A- and B-type maize mutant starches. Carbohydr Res 326:130-144
620 Gidley MJ, Bociek SM (1985) Molecular organization in starches: A 13C CP/MAS NMR study.
621 J Am Chem Soc 107:7040-7044
622 Gidley MJ, Bulpin PV (1987) Crystallization of malto-oligosaccharides at models of the
623 crystalline forms of starch. Carbohydr Res 161:291-300
624 Guan H, Preiss J (1993) Differentiation of the properties of the branching isozymes from maize
625 (*Zea mays*). Plant Physiol 102:1269-1273
626 He W, Lin L, Wang J, Zhang L, Liu Q, Wei C (2018) Inhibition of starch branching enzymes in
627 waxy rice increases the proportion of long-chains of amylopectin resulting in the comb-like
628 profiles of starch granules. Plant Sci 277:177-187
629 He W, Wei C (2020) A critical review on structural properties and formation mechanism of
630 heterogeneous starch granules in cereal endosperm lacking starch branching enzyme. Food
631 Hydrocolloids 100:105434
632 Henmi K, Sato H, Matsuba G, Tsuji H, Nishida K, Kanaya T, Toyohara K, Oda A, Endou K (2016)
633 Isothermal crystallization process of poly(l-lactic acid)/ply(d-lactic acid) blends after rapid
634 cooling from the melt. ACS Omega 1:476-482
635 Hieu HC, Li H, Miyauchi Y, Mizutani G, Fujita N, Nakamura Y (2015) Wetting effect on optical
636 sum frequency generation (SFG) spectra of D-glucose, D-fructose, and sucrose,
637 Spectrochimica Acta A138: 834-839
638 Hizukuri S (1986) Polymodal distribution of the chain lengths of amylopectin, and its significance.
639 Carbohydr Res 147:342-347
640 Horie T, Shiraiwa T, Homma K, Katsura K, Maeda S, Yoshida H (2005) Can yields of lowland
641 rice resume the increases that they showed in the 1980s? Plant Prod Sci 8:259-274

642 Imberty A, Buléon A, Tran V, Tran V, Pérez S (1991) Recent advances in knowledge of starch
643 structure. Starch/Stärke 43:375-384
644 Jane JL, Wong KS, McPherson AE (1997) Branch-structure difference in starches of A- and B-
645 type X-ray patterns revealed by their Naegeli dextrins. Carbohydr Res 300:219-227
646 Kainuma K, French D (1972) Naegeli amylodextrin and its relationship to starch granule
647 structure. II. Role of water in crystallization of B-starch. Biopolym 11:2241-2250
648 Kikumoto S, French D (1983) Naegeli amylodextrin: Large scale preparation of fractions by
649 step-wise precipitation using organic solvents. J Jpn Soc Starch Sci 30:69–75
650 Kong L, Lee C, Kim SH, Ziegler GR (2014) Characterization of starch polymorphic structures
651 using vibrational sum frequency generation spectroscopy. J Phys Chem B 118:1775-1783
652 Matsuki J, Wada M, Sasaki T, Yoza K, Tokuyasu K (2019) Purification of branched dexrin from
653 Nägeli amylodextrin by ethanol precipitation and characterization of its aggregation property
654 by methanol-water. J Appl Glycosci 66:97-102
655 Matsushima R, Maekawa M, Kusano M, Tomita K, Kondo H, Nishimura H, Crofts N, Fujita N,
656 Sakamoto W (2016) Amyloplast membrane protein SUBSTANDARD STARCH GRAIN6
657 controls starch grain size in rice endosperm. Plant Physiol 170:1445-1459
658 Matsushima R, Maekawa M, Sakamoto W (2015) Geometrical formation of compound starch
659 grains in rice implements Voronoi diagram. Plant Cell Physiol 56:2150-2157
660 Miyauchi Y, Sano H, Mizutani G (2006) Selective observation of starch in a water plant using
661 optical sum-frequency microscopy. J Opt Soc Am A 23:1687-1690
662 Morita R, Crofts N, Shibatani N, Miura S, Hosaka Y, Oitome NF, Ikeda K, Fujita N, Fukayama
663 H (2019) CO2-responsive CCT protein stimulates the ectopic expression of particular starch
664 biosynthesis-related enzymes, which markedly change the structure of starch in the leaf sheaths
665 of rice. Plant Cell Physiol 60:961-972
666 Nagasaki A, Matsuba G, Ikemoto Y, Moriwaki T, Ohta N, Osaka K (2021) Analysis of the sol and
667 gel structures of potato starch over a wide spatial scale. Food Sci Nutr 9:4916-4926
668 Nakamura Y (2002) Towards a better understanding of the metabolic system for amylopectin
669 biosynthesis in plants: Rice endosperm as a model tissue. Plant Cell Physiol 43:718-725
670 Nakamura Y (2015) Biosynthesis of reserve starch. In: Nakamura Y (ed) Starch: Metabolism and
671 Structure. Springer, Tokyo, Heidelberg, New York, Dordrecht, London, pp 161-209
672 Nakamura Y (2018) Rice starch biotechnology: Rice endosperm as a model of cereal endosperms.
673 Starch 70:1600375
674 Nakamura Y, Aihara S, Crofts N, Sawada T, Fujita N (2014) *In vitro* studies of enzymatic
675 properties of starch synthases and interactions between starch synthase I and starch branching
676 enzymes in rice. Plant Sci 224:1-8

677 Nakamura Y, Kainuma K (2021) On the cluster structure of amylopectin. Plant Mol Biol
678 Published online: 02 October 2021
679 Nakamura Y, Ono M, Hatta T, Kainuma K, Yashiro K, Matsuba G, Matsubara A, Miyazato A,
680 Mizutani G (2020a) Effects of BEIIb-deficiency on the cluster structure of amylopectin and the
681 internal structure of starch granules in endosperm and culm of *japonica*-type rice. Front Plant
682 Sci 11:571346
683 Nakamura Y, Ono M, Suto M, Kawashima H (2020b) Analysis of malto-oligosaccharides and
684 related metabolites in rice endosperm during development. Planta 241:110
685 Nakamura Y, Yuki K, Park SY, Ohya T. (1989) Carbohydrate metabolism in the developing
686 endosperm of rice grains. Plant Cell Physiol 30:833-839
687 Nakamura Y, Sakurai A, Inaba Y, Kimura K, Iwasawa N, Nagamine T (2002) The fine structure
688 of amylopectin in endosperm from Asian cultivated rice can be largely classified into two
689 classes. Starch 54:117-131
690 Nishi A, Nakamura Y, Tanaka N, Satoh H (2001) Biochemical and genetic analysis of the effects
691 of *amylose-extender* mutation in rice endosperm. Plant Physiol 127:459-472
692 Ohdan, T., Francisco, Jr. P.B., Sawada, T., Hirose, T., Terao, T., Satoh, H., *et al*. (2005) Expression
693 profiling of genes involved in starch synthesis in sink and source organs of rice. J Exp Bot 56:
694 3229-3244
695 O'Shea MG, Samuel MS, Konik CM, Morell MK (1998) Fluorophore-assisted carbohydrate
696 electrophoresis (FACE) of oligosaccharides: Efficiency of labeling and high-resolution
697 separation. Carbohydr Res 307:1-12
698 Peat S, Whelan WJ, Thomas GJ (1952) Evidence of multiple branching in waxy maize starch. J
699 Chem Soc 4546-4548
700 Satoh H, Nishi A, Yamashita K, Takemoto Y, Tanaka Y, Hosaka Y et al (2003a) Starch-branching
701 enzyme I-deficient mutation specifically affects the structure and properties of starch in rice
702 endosperm. Plant Physiol 133:1111-1121
703 Satoh H, Nishi A, Fujita N, Kubo A, Nakamura Y, Kawasaki T, Okita TW (2003b) Isolation and
704 characterization of starch mutants in rice. J Appl Glycosci 50:223-230
705 Sawada T, Nakamura Y, Ohdan T, Saitoh A, Francisco Jr, PB, Suzuki E, et al. (2014) Diversity of
706 reaction characteristics of glucan branching enzymes and the fine structure of α-glucan from
707 various sources. Arch Biochem Biophys 562:9-21
708 Sawada T, Itoh M, Nakamura Y (2018) Contributions of three starch branching enzyme isozymes
709 to the fine structure of amylopectin in rice endosperm. Front Plant Sci 01536
710 Shannon JC, Garwood DL, Boyer CD (2009) Genetics and physiology of starch development. In:
711 BeMiller J, Whistler R (ed) In Starch, Chemistry and Technology, 3rd edn. Academic Press,
712 New York, pp 23-82

Tanaka N, Fujita N, Nishi A, Satoh H, Hosaka Y, Ugaki M, Kawasaki S, Nakamura Y (2004) The structure of starch can be manipulated by changing the expression levels of starch branching enzyme IIb in rice endosperm. Plant Biotechnol J 2:507–516

Tetlow IJ, Emes MJ (2017) Starch biosynthesis in the developing endosperms of grasses and cereals. Agronomy 7:1

Thompson DB (2000) On the non-random nature of amylopectin branching. Carbohydr Polym 43:223-239

Toyosawa Y, Kawagoe Y, Matsushima R, Crofts N, Ogawa M, Fukuda M, Kumamaru T, Okazaki Y, Kusano M, Saito K, Toyooka K, Sato M, Ai Y, Jane JL, Nakamura Y, Fujita N (2016) Deficiency of starch synthase IIIa and IVb alters starch granule morphology from polyhedral to spherical in rice endosperm. Plant Physiology 170:1255-1270

Wei C, Xu B, Qin F, Yu H, Chen C, Meng X, Zhu L, Wang Y, Gu M, Liu Q (2010) C-type starch from high-amylose rice resistant starch granules modified by antisense RNA inhibition of starch branching enzyme. Agric Food Chem 58:7383-7388.

Yamaguchi M, Kainuma K, French D (1979) Electron microscopic observations of waxy maize starch. J Ultrastr Res 69:249-261

Yamanouchi H, Nakamura Y (1992) Organ specificity of isoforms of starch branching enzyme (Q-enzyme) in rice. Plant Cell Physiol 33:985-991

Yano M, Okuno K, Kawakami J, Satoh H, Omura T 1985 High amylose mutants of rice, *Oryza sativa* L. Theor Appl Genet 69:253-257

Legends for figures

Fig. 1. Native-PAGE/activity staining of BE isozymes in developing endosperms and culms from the wild-type *japonica* rice cultivars Kinmaze and Taichung-65, a *be2a* mutant line, EM19, a *be2b* mutant line, EM10, and a *be1* mutant line, EM557.
a, Activity levels of BE isozymes in developing endosperms at 15-20 DAP. Lanes: 1, Kinmaze; 2, EM19; 3, EM10; 4, EM557; 5, Taichung-65. The volume of each crude enzyme extract applied was 1.3 µl. b, Activity levels of BE isozymes in the culm. Lanes: 1, Kinmaze; 2, EM19; 3, EM557. The volume of each crude enzyme extract applied was 8.6 µl. In b, positions of BE isozymes on the gel were shown by comparing those in the endosperm, being consistent with our previous study (Yamanouchi and Nakamura 1992). The experiments were repeated at least three times until all these results were consistent, whereas each figure shows one representative result.

Fig. 2. Chain-length distribution of amylopectin in developing endosperms of the wild-type *japonica* cultivar Kinmaze and a *be2b* mutant line, EM10. The vertical axis presents the proportion (molar %) of the amount of each chain to the total amounts of chains with degree of polymerization (DP) from 3 to 80, whereas the horizontal axis shows the DP value of the chain.
a, Amylopectin in 4-6 DAP endosperm from Kinmaze; b, Amylopectin in 15-20 DAP endosperm from Kinmaze; c, Amylopectin in DAP4-6 endosperm from EM10; d, Amylopectin in 15-20 DAP endosperm from EM10. e, Difference between EM10 amylopectin in endosperm at 4-6 DAP and Kinmaze amylopectin at 15-20 DAP, calculated from data of the former subtracted by those of the latter. f, Difference between EM10 amylopectin in endosperm at 15-20 DAP and Kinmaze amylopectin at 15-20 DAP, calculated from data of the former subtracted by those of the latter. The experiments were repeated at least three times until all these results were consistent, whereas each figure shows one representative result. Values are the averages calculated from three replicate measurements. Standard deviations were too small to be shown in the figure.

Fig. 3. Chain-length distribution of amylopectin in the culms of the wild-type *japonica* cultivar Kinmaze and a *be2a* mutant line, EM19, a *be2b* mutant line, EM10, and a *be1* mutant line, EM557. The vertical axis presents the proportion (molar %) of the amount of each chain to the total amounts of chains with degree of polymerization (DP) from 3 to 80 whereas the horizontal axis shows the DP value of the chain.
a, Amylopectin in the culm from Kinmaze; b, Amylopectin in the culm from EM19; c, Amylopectin in the culm from EM10. d, Amylopectin in the culm from EM557. e, Difference in

the EM10 culm amylopectin, calculated from data of EM10 subtracted by those of Kinmaze. f, Difference in the EM19 culm amylopectin, calculated from data of EM19 subtracted by those of Kinmaze. The other conditions are the same as in Fig. 2.

Fig. 4. Gel filtration chromatogram of isoamylase-debranched starch in the culm from Kinmaze and EM19.

a, Kinmaze. b, EM19. Glucans were classified into 3 fractions according to the procedure by Toyosawa et al. (2016); Fraction I including amylose and extra-chains of amylopectin, if any; Fraction 2, cluster-interconnecting chains (B2-4 chains); Fraction 3, short chains (A plus B1 chains). The numbers expressed in parenthesis in 3 fractions mean the amounts of carbohydrates as percentages of total carbohydrates in starches. The chromatography was repeated three times until all these results were consistent, whereas each figure shows one representative result.

Fig. 5. Wide angle X-ray scattering (WAXS) analysis of starch granules in mature endosperms from the wild-type *japonica* cultivars Kinmaze and Taichung65, a *be2a* mutant line, EM19, a *be2b* mutant line, EM10, a *be1* mutant line, and EM557, and standard glucans having the A-type allomorph BD4A and the B-type allomorph BD4B.

a, Standard glucans, BD4A (solid line) and BD4B (dotted line). b-f, Starch granules in mature endosperm: Kinmaze (b), Taichung65 (c), EM19 (d), EM10 (e), and EM557 (f). The experiments were repeated at least three times until all these results were consistent, whereas each figure shows one representative result.

Fig. 6. Wide angle X-ray scattering (WAXS) analysis of starch granules in developing endosperms from the wild-type *japonica* cultivars Kinmaze and a *be2b* mutant line, EM10, and starch granules in the culm from Kinmaze and a *be2a* mutant line, EM19.

a, Starch granules in 4-6 DAP endosperms from Kinmaze. b, Starch granules in 4-6 DAP endosperms from EM10. c, Starch granules in 15-20 DAP endosperms from Kinmaze. d, Starch granules in 15-20 DAP endosperms from EM10. e, Starch granules in the culm from Kinmaze. f, Starch granules in the culm from EM19. The other conditions are the same as in Fig. 4.

Fig. 7. SFG spectra of starch granules in mature endosperms from the wild-type *japonica* cultivar Kinmaze, a *be2a* mutant line, EM19, a *be2b* mutant line, EM10, a *be1* mutant line, and EM557, and standard glucans having the A-type allomorph BD4A and the B-type allomorph BD4B.
a, Standard glucans, BD4A. b, Standard glucans, BD4B. c-f, Starch granules in mature endosperm: Kinmaze (c), EM19 (d), EM10 (e), and EM557 (f). The experiments were repeated at least three times until all these results were consistent, whereas each figure shows one representative result.

Fig. 8. SFG spectra of starch granules in developing endosperms from the wild-type *japonica* cultivars Kinmaze and a *be2b* mutant line, EM10, and starch granules in the culm from Kinmaze and a *be2a* mutant line, EM19.
a, Starch granules in 4-6 DAP endosperms from Kinmaze. b, Starch granules in 4-6 DAP endosperms from EM10. c, Starch granules in 15-20 DAP endosperms from Kinmaze. d, Starch granules in 15-20 DAP endosperms from EM10. e, Starch granules in the culm from Kinmaze. f, Starch granules in the culm from EM19. The other conditions are the same as in Fig. 6.

Fig. 9. A schematic representation of the hypothetical cluster structure of amylopectin in endosperm from the wild-type *japonica* rice cultivar Kinmaze compared with that of a *be2b* (*ae*) mutant line EM10 and that in the culm from Kinmaze and a *be2a* mutant line EM19. According to the past and present studies, we hypothesize that branch points are located in two separate zones which are mainly formed by BEI and BEIIb (a) in the endosperm and BEI and BEIIa in the culm (b), respectively. The first branch points are localized in the amorphous lamellae whereas the second branch points are localized in the reducing part of the crystalline lamellae, and presumably, in addition the intermediate region between both lamellae. Note that in the absence of BEIIb in the endosperm, amylopectin structure becomes the B-type from the A-type in the wild-type whereas in the culm, amylopectin shifts to the B-type in the absence of BEIIa from the A-type in the wild-type amylopectin.

Fig. 10. Comparison of chain-length distribution of amylopectin among developing and mature endosperm and the culms from the wild-type *japonica* cultivar Kinmaze, a *be2a* mutant line, EM19, and a *be2b* mutant line, EM10. The vertical axis presents difference in the proportion (molar %) of the amount of each chain to the total amounts of chains with degree of polymerization (DP) from 3 to 80 whereas the horizontal axis shows the DP value of the chain.

a, Difference between amylopectin from mature endosperm, calculated from data of EM10 subtracted by those of Kinmaze. b, Difference between amylopectin from 4-6 DAP EM10 endosperm and mature Kinmaze endosperm, calculated from data of the former subtracted by the latter. c, Difference between amylopectin from 15-20 DAP EM10 endosperm and mature Kinmaze endosperm, calculated from data of the former subtracted by the latter. d, Difference between amylopectin from the EM19 culm and mature Kinmaze endosperm, calculated from data of the former subtracted by the latter. The other conditions are the same as in Fig. 2.

Table 1

Summary of crystalline polymorphs of starch granules in mature endosperm, developing endosperm, and culm from the wild-type *japonica* rice cultivars Kinmaze and Taichung65, *be2a* mutant, *be2b* mutant, and *be1* mutant lines.

(Experiment I)

Cultivar	Genotype	Mature endosperm
Kinmaze	WT	A
Taichung65	WT	A
EM19	*be2a*	A
EM10	*be2b*	B
EM557	*be1*	A

(Experiment II)

Cultivar	4-6 DAP endosperm			15-20 DAP endosperm			Culm		
	CLD	XRD	SFG	CLD	XRD	SFG	CLD	XRD	SFG
Kinmaze	A	A	A	A	A	A	A	A	A
EM19	-	-	-	-	-	-	B	B'(A)	B(A)
EM10	A	A	A(B)	B	B'(A)	B	-	-	-

CLD, chain-length distribution pattern of amylopectin. B', the pattern with a significant similarity to that of B-type starch. (A) or (B), the pattern suggesting co-existence of A-type or B-type starch. See details in the text.

927 Title for Supplementary Fig. S1.
928 Principal component analysis (PCA) of optical sum frequency generation spectra in the CH
929 stretching region of various types of amylopectin in starch granules modified by branching
930 enzyme mutations of *japonica* rice. The top narrow panel is the projection of the lower panel onto
931 the PC1 axis.
932
933
934
935 Title for Supplementary Table S1.
936 Parameters used for fitting the SFG spectra of starch granules to the theoretical curve in Eq. (1).
937
938
939

Fig. 1

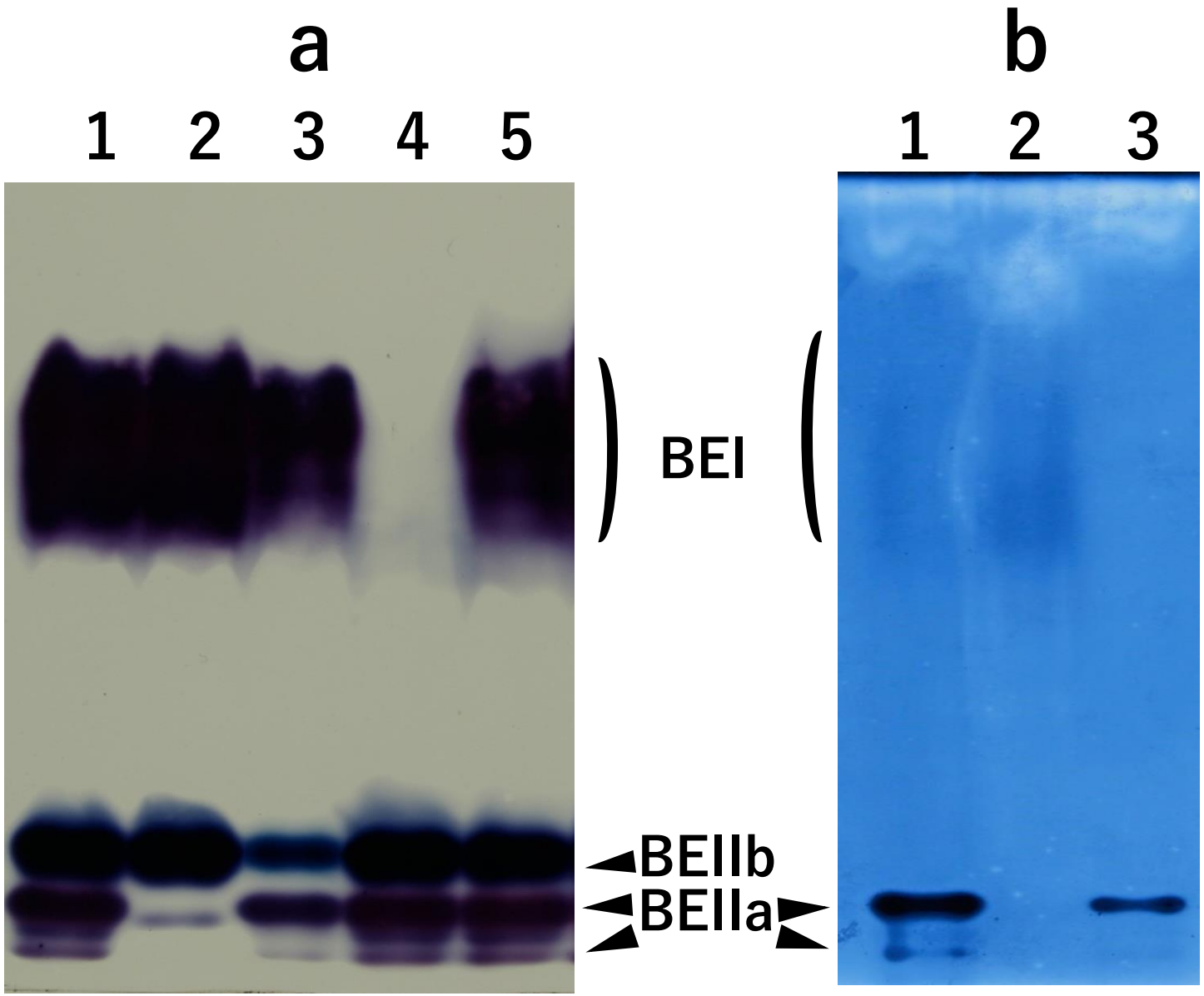

Fig. 2

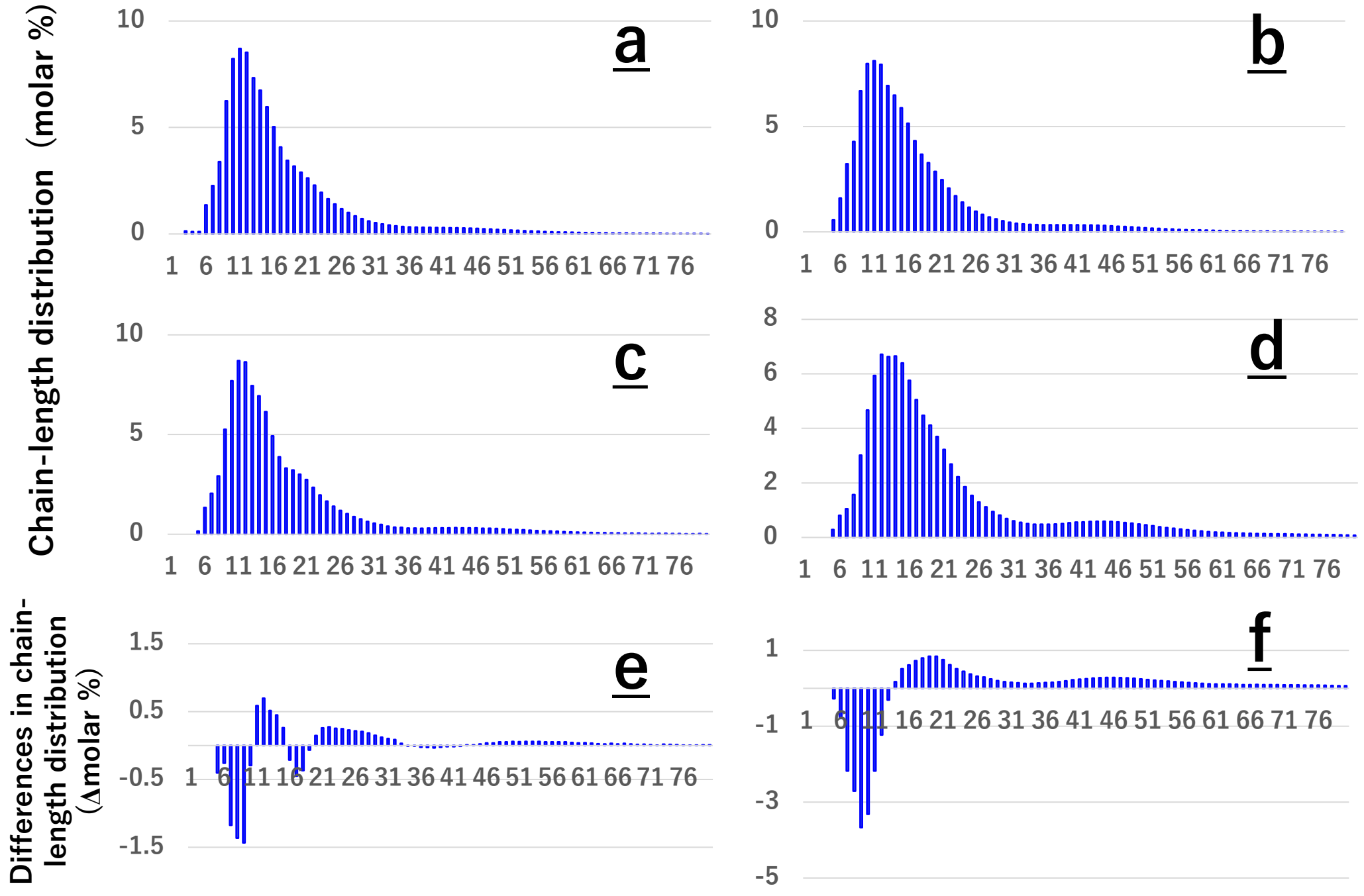
Chain-length distribution (molar %)
a
b
c
d
e
f
Differences in chain-length distribution (Δmolar %)
1 6 11 16 21 26 31 36 41 46 51 56 61 66 71 76

Fig. 3

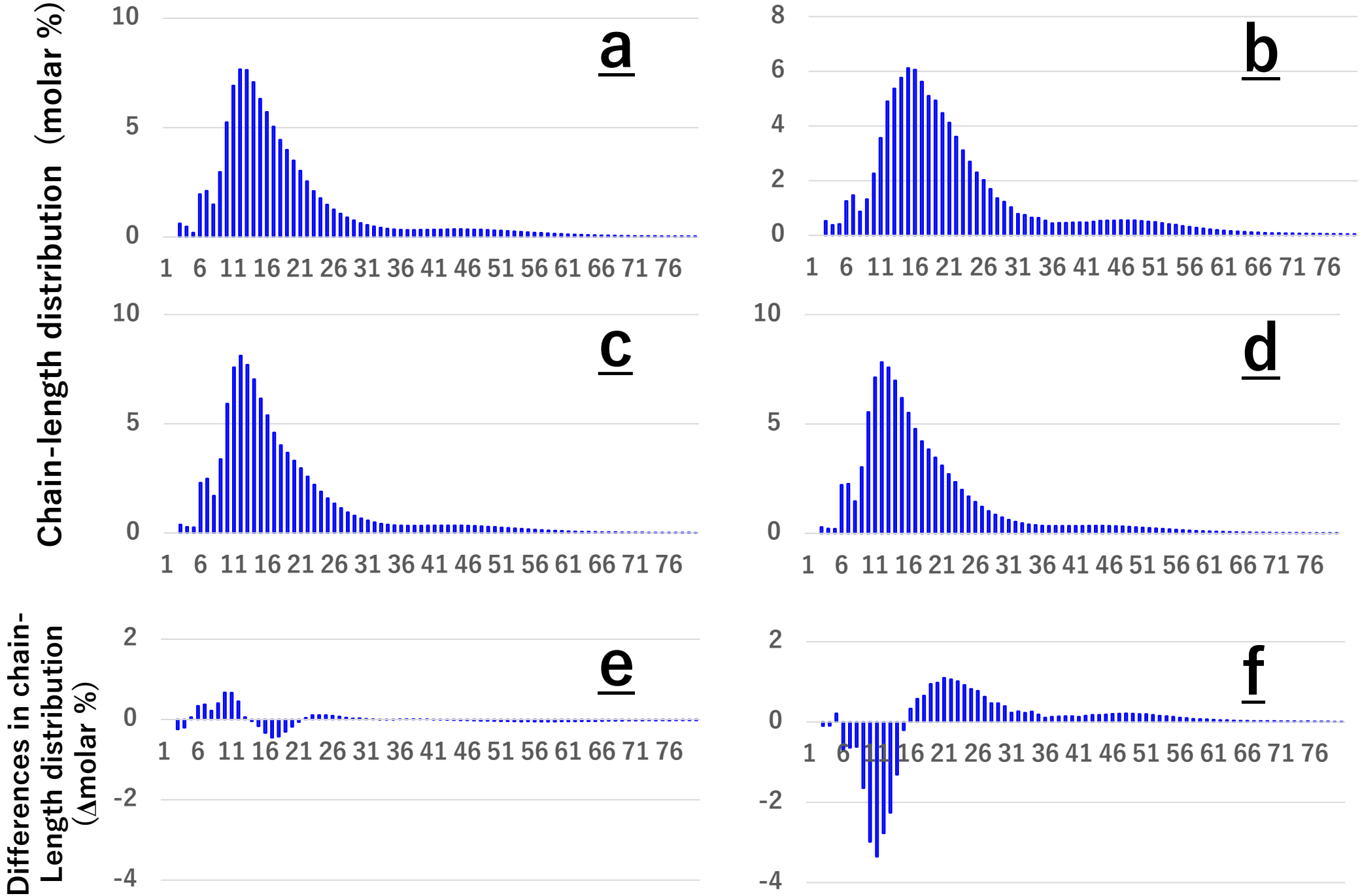
Chain-length distribution (molar %)
a
b
c
d
e
f
Differences in chain-Length distribution (Δmolar %)
1 6 11 16 21 26 31 36 41 46 51 56 61 66 71 76

Fig. 4

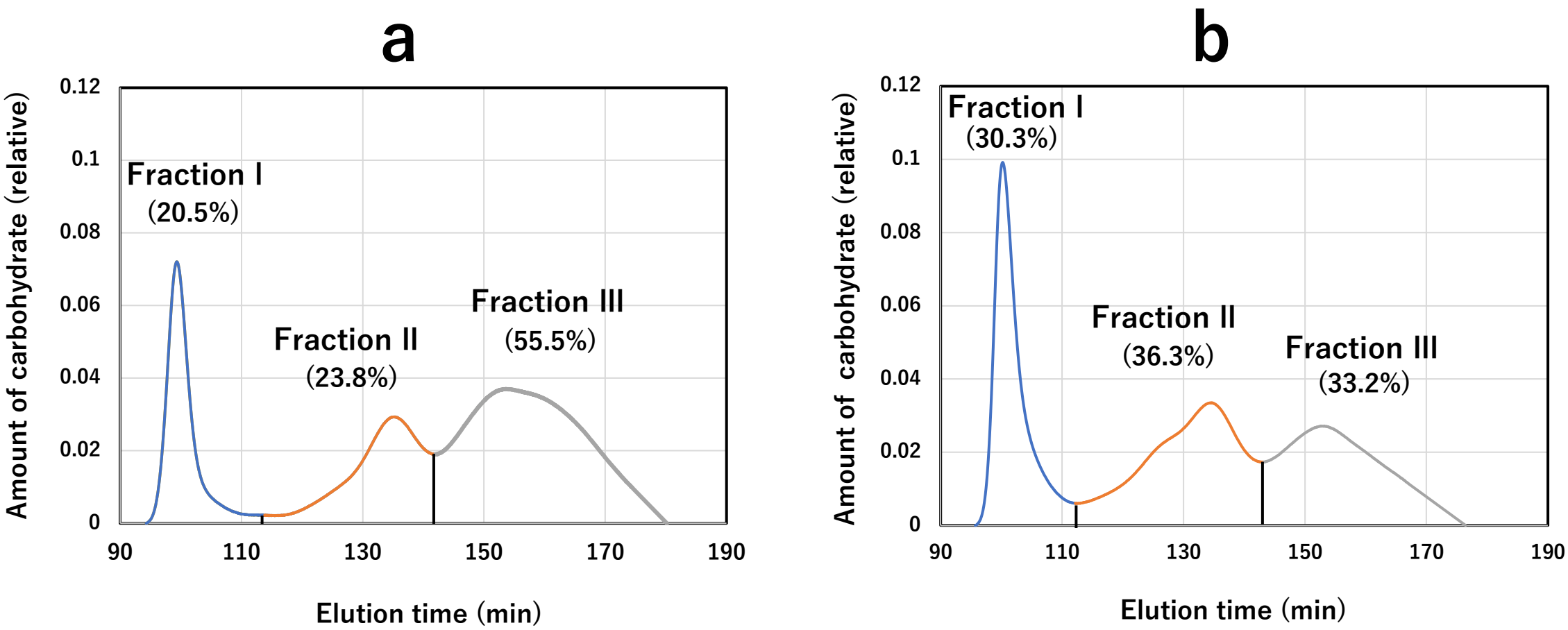
a
Amount of carbohydrate (relative)
0.12
0.1
0.08
0.06
0.04
0.02
0
Fraction I
(20.5%)
Fraction II
(23.8%)
Fraction III
(55.5%)
90
110
130
150
170
190
Elution time (min)
b
Amount of carbohydrate (relative)
0.12
0.1
0.08
0.06
0.04
0.02
0
Fraction I
(30.3%)
Fraction II
(36.3%)
Fraction III
(33.2%)
90
110
130
150
170
190
Elution time (min)

Fig. 5

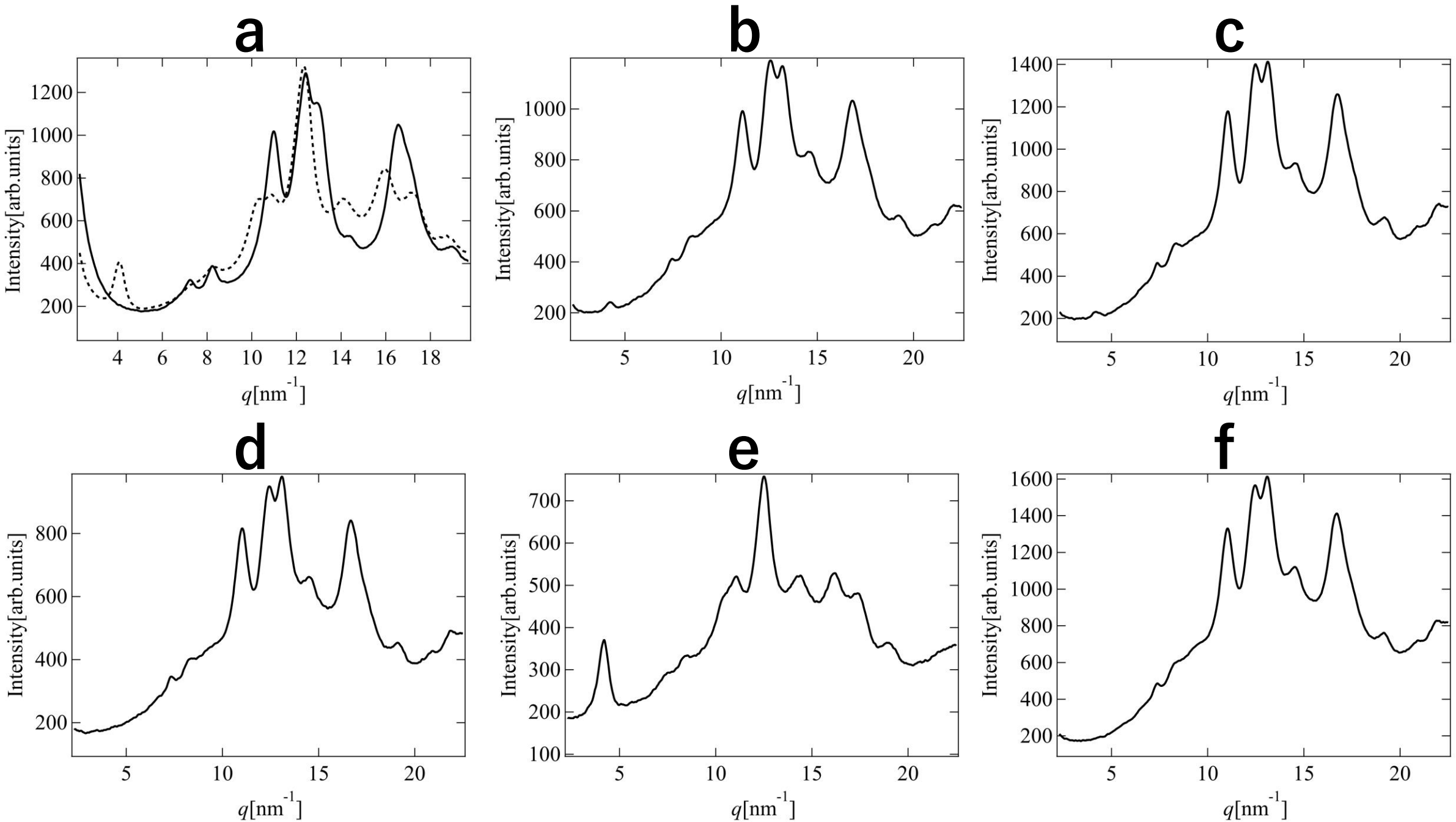

Fig. 6

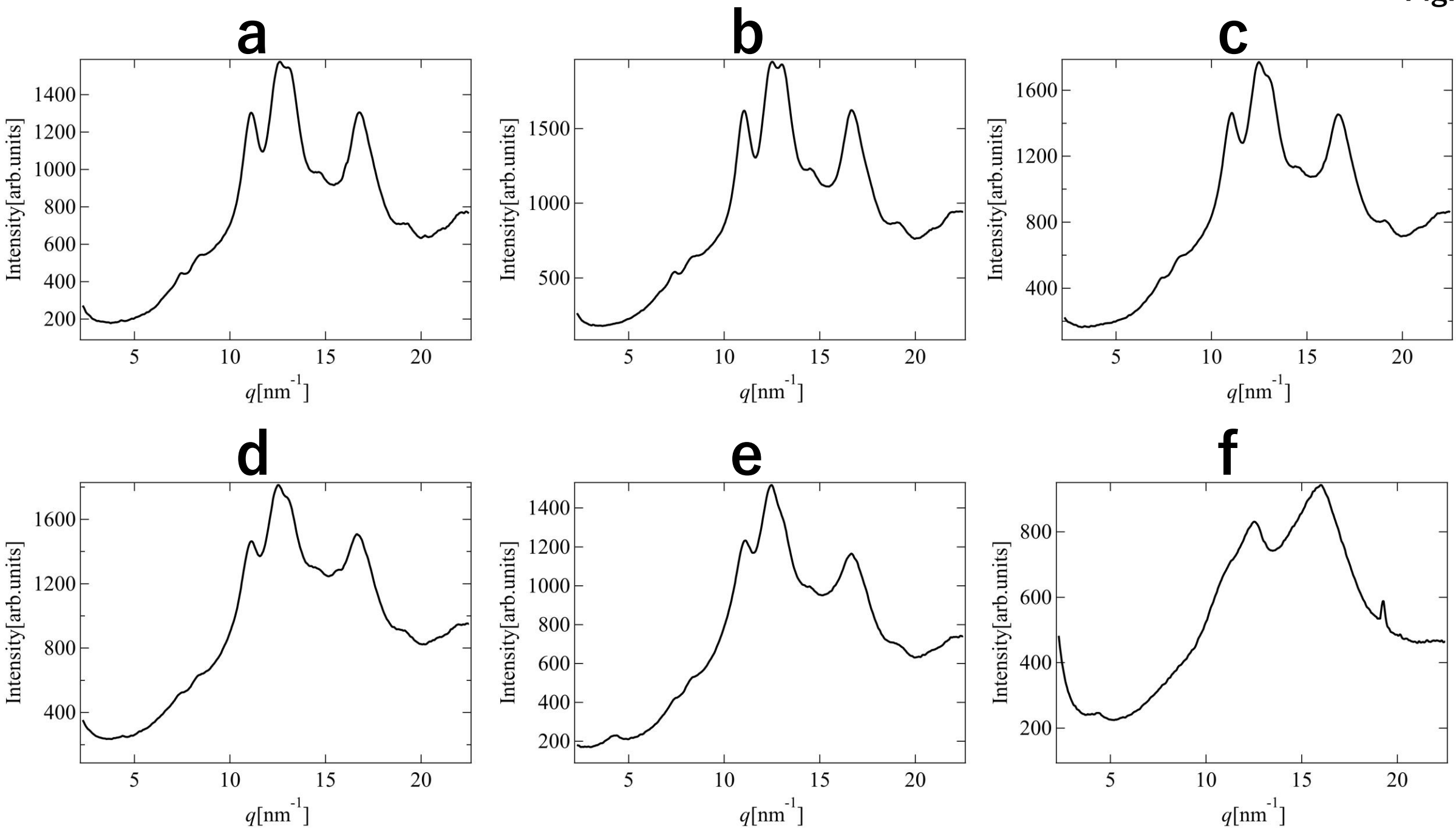

Fig. 7

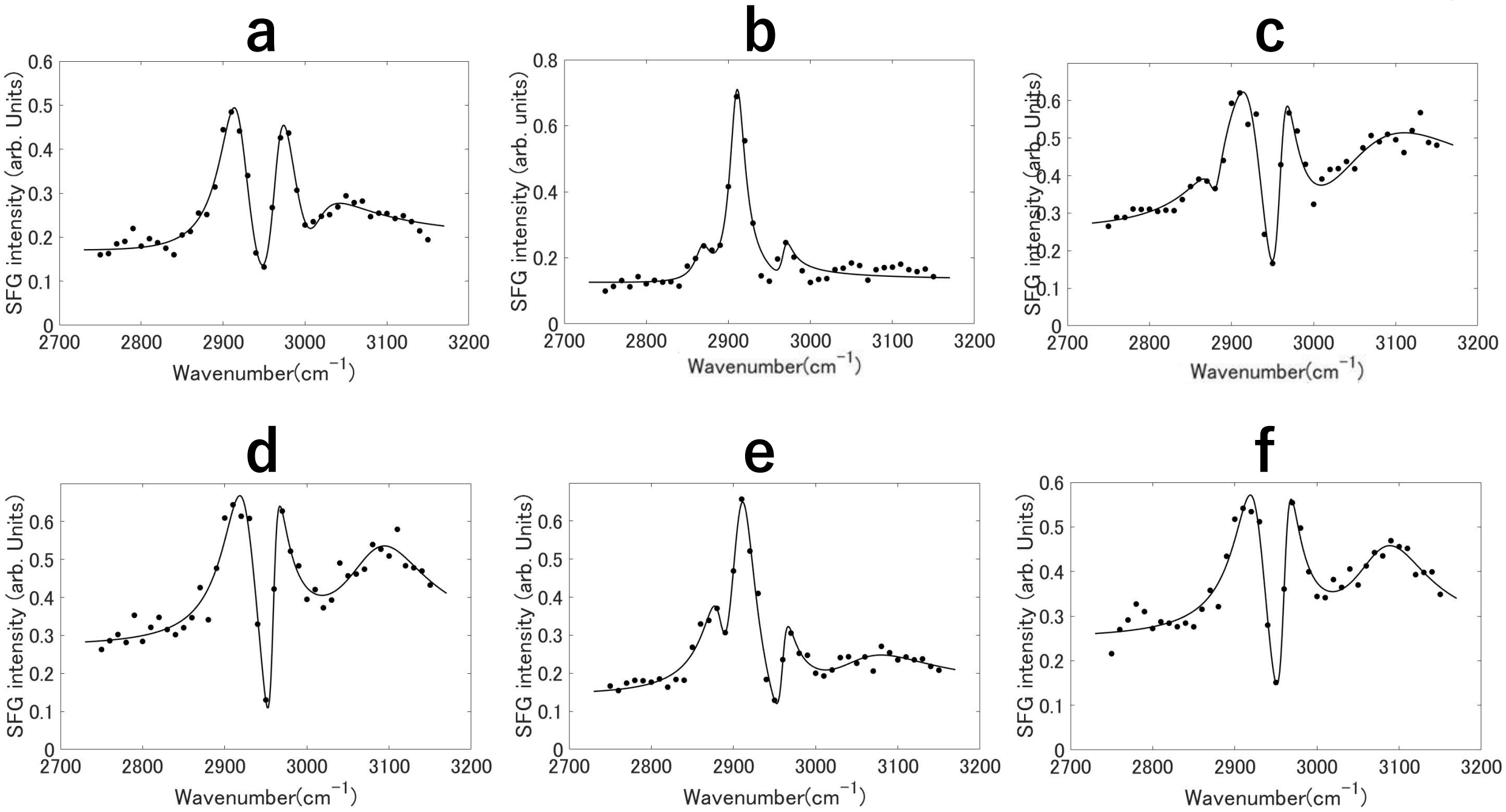
a
b
c
d
e
f
SFG intensity (arb. Units)
SFG intensity (arb. units)
Wavenumber(cm^{-1})
2700
2800
2900
3000
3100
3200

Fig. 8

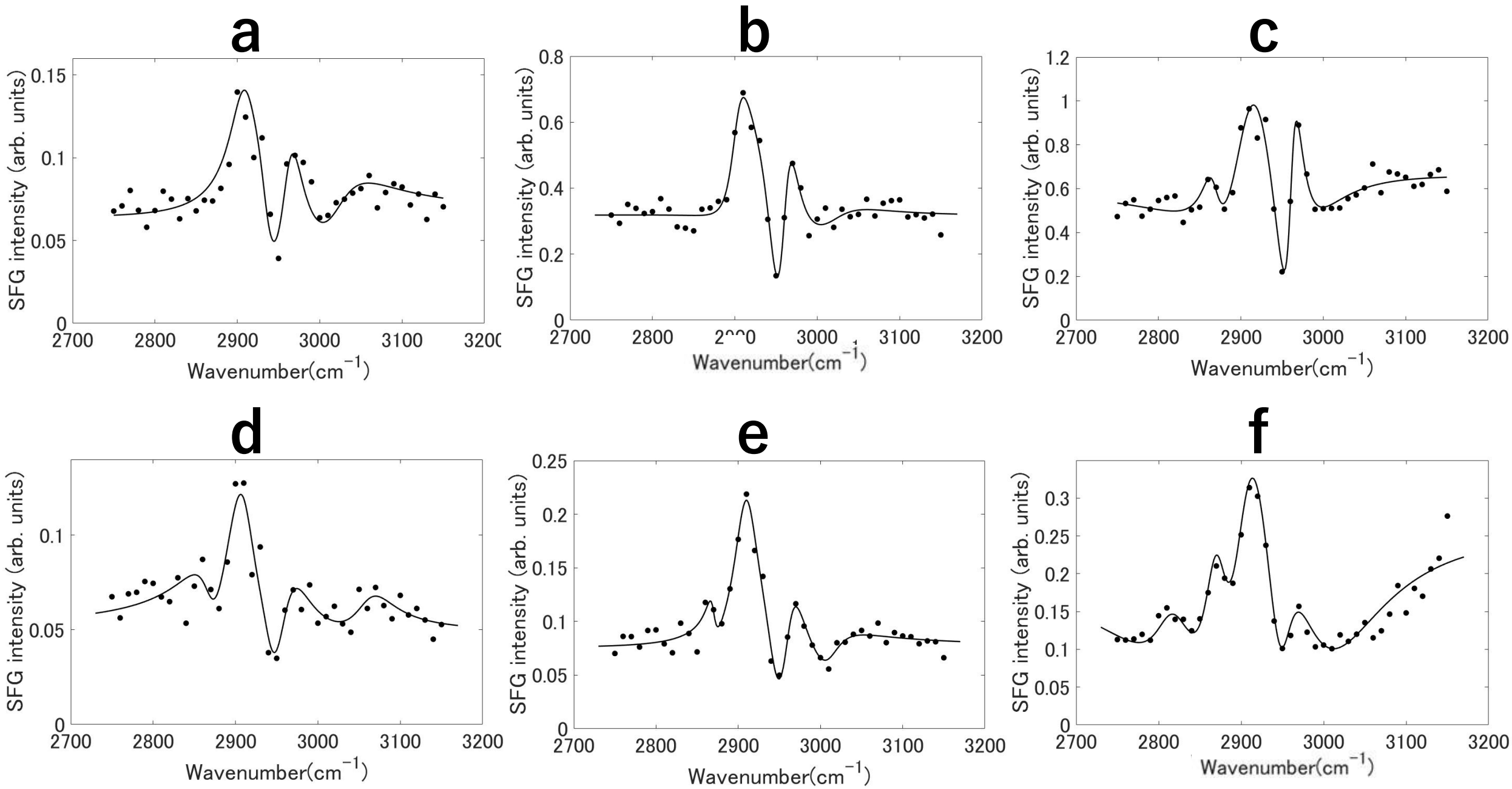
a
b
c
d
e
f
SFG intensity (arb. units)
Wavenumber(cm^{-1})
2700
2800
2900
3000
3100
3200

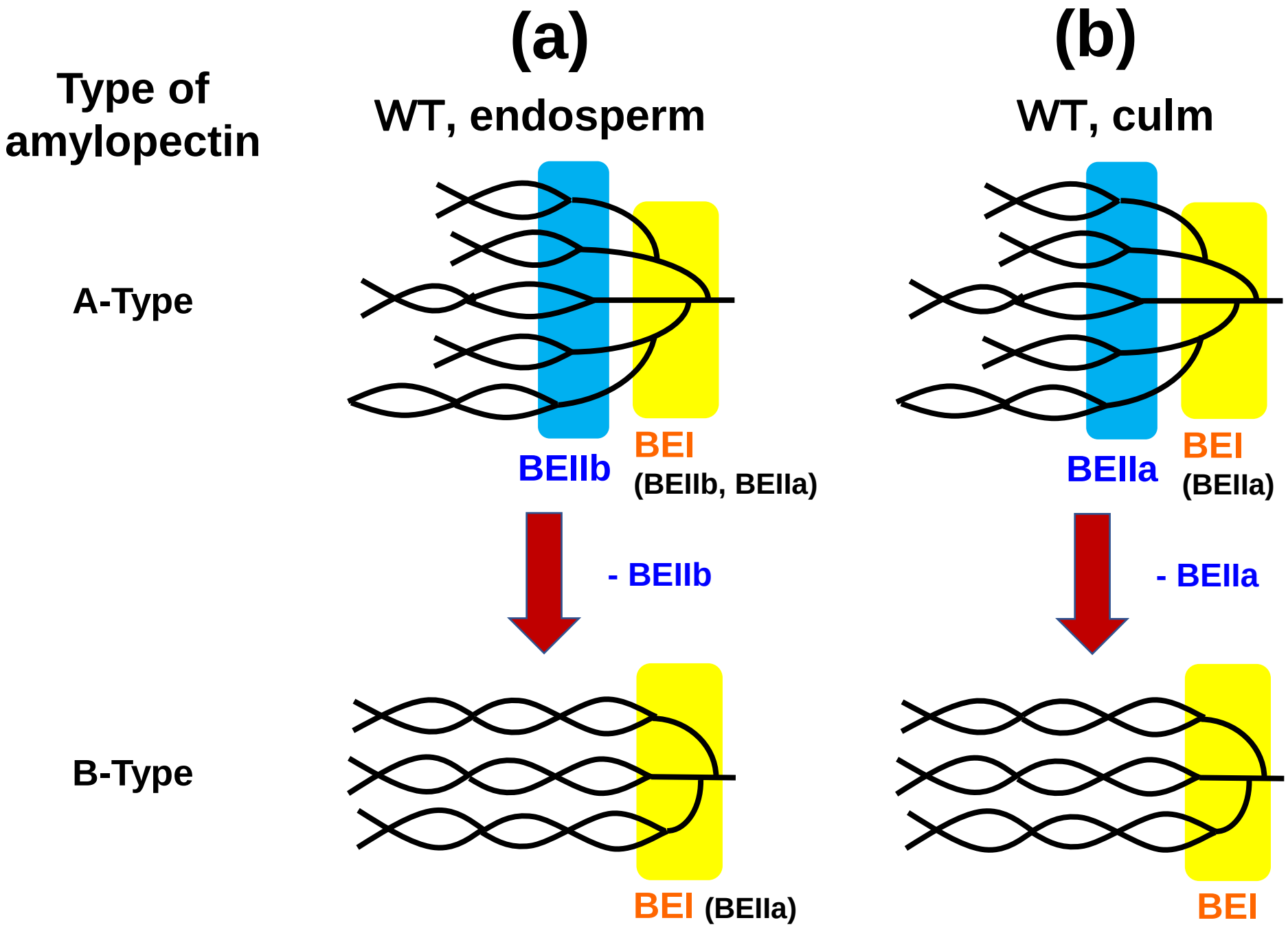
Type of amylopectin
(a)
WT, endosperm
(b)
WT, culm
A-Type
BEIIb
BEI
(BEIIb, BEIIa)
BEIIa
BEI
(BEIIa)
- BEIIb
- BEIIa
B-Type
BEI (BEIIa)
BEI

Fig. 10

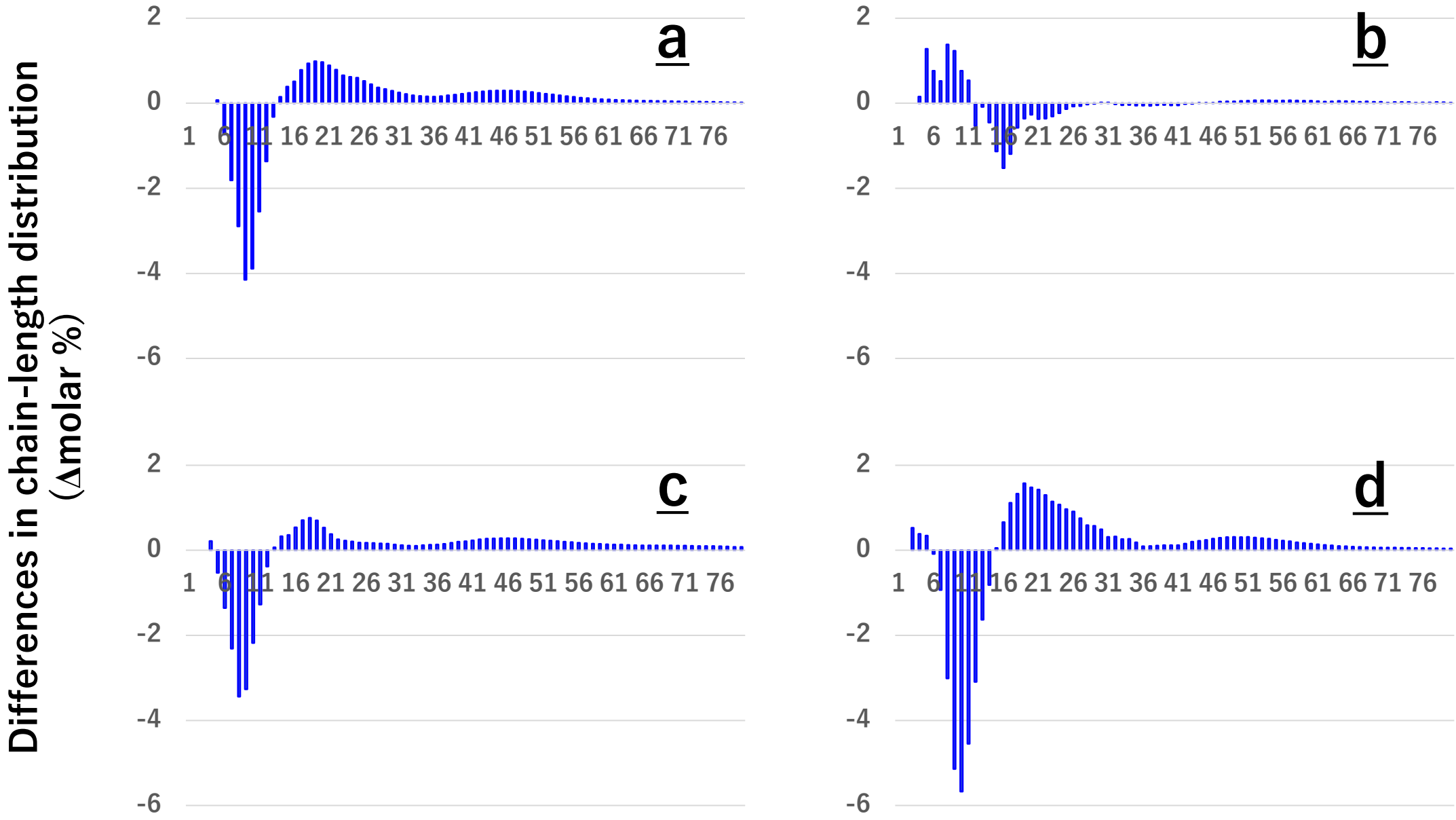
Differences in chain-length distribution
(Δmolar %)
a
b
c
d
2
0
-2
-4
-6
1 6 11 16 21 26 31 36 41 46 51 56 61 66 71 76

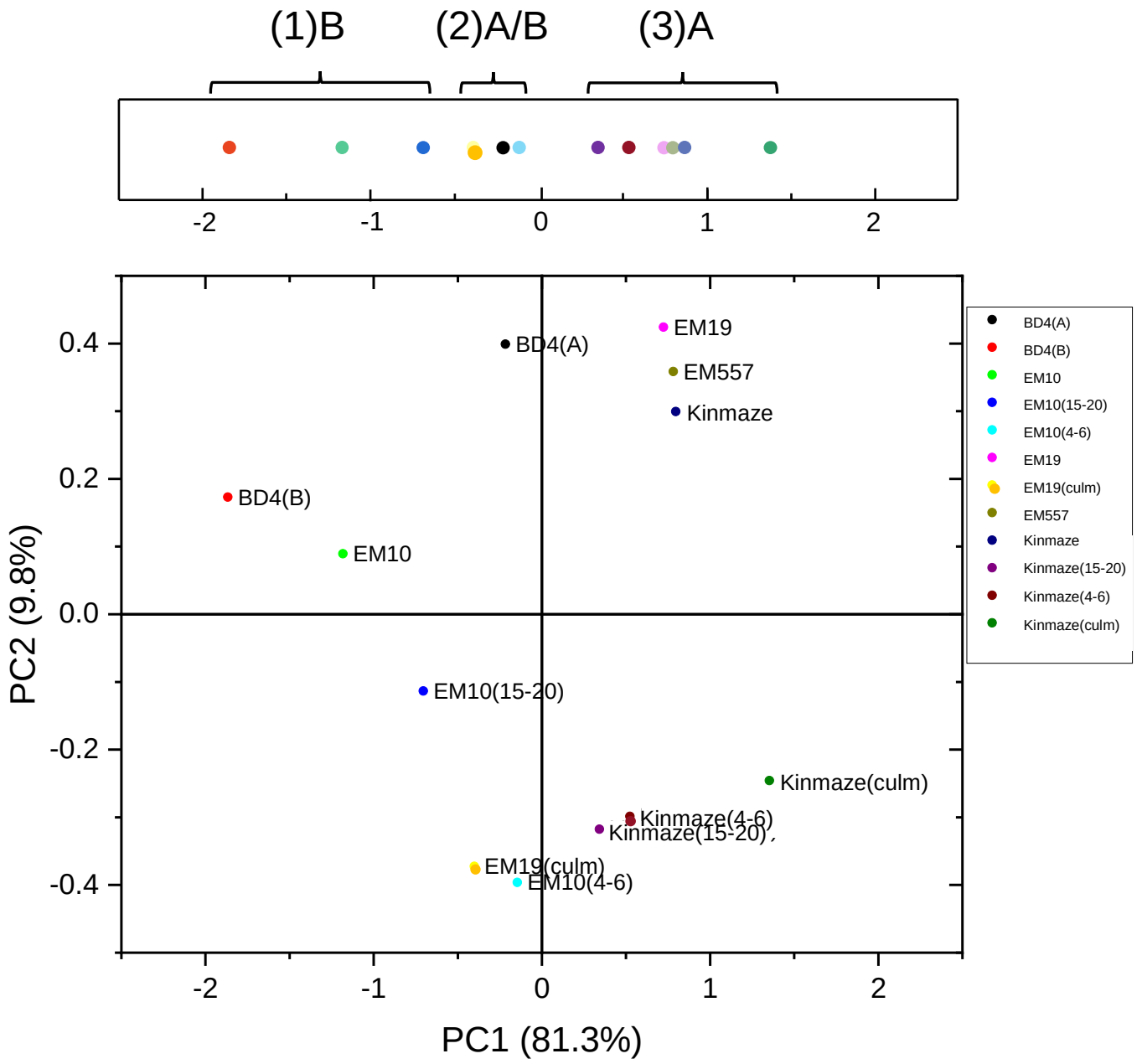

Supplementary Figure S1. Principal component analysis (PCA) of optical sum frequency generation spectra in the CH stretching region of various types of amylopectin in starch granules modified by branching enzyme mutations of *japonica* rice. The top narrow panel is the projection of the lower panel onto the PC1 axis.

Supplementary Table S1. Parameters used for fitting the SFG spectra of starch granules to the theoretical curve in Eq. (1).

		BD4A	BD4B	Kinmaze	EM10	EM19	EM557	EM10(DAP4-6)	EM10(DAP15-20)	EM19(culm)	Kinmaze(DAP4-6)	Kinmaze(DAP15-20)	Kinmaze(culm)
Nonresonant susceptibility (arbitrary units)	χ_{NR}	0.431	0.3625	0.5356	0.3895	0.564	0.522	0.224	0.2764	0.4907	0.2576	0.5622	0.7962
Amplitude (arbitrary units)	A1		1.184	0.9123	3.301	0.386	0.158	13.51	4.515	12.09	14.57	23.6	16.71
	A2	11.29	5.514	19.72	11.68	13.41	9.001	10.21	15.19	32.98	53.66	18.89	32.04
	A3	11.87	0.8259	5.97	2.161	4.83	3.493	12.62	3.997	6.553	43.57	10.11	28.8
	A4	28.92		38.44	7.694	11.17	6.494	17.05	2.014	50.17	3.713	3.259	7.24
	A5							3.854	4.062	6.973			
Resonant wavenumber (cm^{-1})	ω_1		2869	2880	2885	2880	2880	2870	2870	2870	2897	2903	2867
	ω_2	2919	2910	2929	2910	2920	2920	2911	2910	2901	2952	2950	2904
	ω_3	2966	2968	2960	2960	2960	2960	2960	2961	2951	2960	2961	2960
	ω_4	3006		3050	3050	3050	3078	3061	3010	2976	3023	3020	2962
	ω_5							2940	2942	2814			
Width (cm^{-1})	γ_1		11.25	9.677	13.09	4	3.248	18.81	6.17	18.62	17.88	15.9	13.38
	γ_2	23.62	11.43	32.83	20.14	30.84	28.2	23.18	18.23	34.69	39.51	24.43	36.07
	γ_3	18.14	7.426	12.11	8.284	10	2960	25.43	16.18	20.6	28.6	13.97	39.94
	γ_4	26.4		-105.9	69.24	58.99	3078	29.94	24.94	89.16	36.05	43.45	10.03
	γ_5							17.8	18.65	29.76			
Phase (rad)	θ_1		1.311	1.321	3.28	2.393	2.03	0.5306	0.6526	0.04821	0.8551	1.372	2.025
	θ_2	5.426	1.311	3.171	4.889	4.633	4.553	2.524	1.925	0.401	3.612	3.411	0.02274
	θ_3	4.423	0.6595	5.153	6.204	0.198	0.195	1.414	0.5574	1.174	0.6413	0.002383	2.539
	θ_4	1.976		0.1785	5.669	6.043	5.223	2.625	1.446	2.222	0.6473	0.03259	0.06886
	θ_5							0.06216	4.49	4.391			